Dear Editor Prof. Ulrike Lohmann

Please find below our responses to the reviewers' comments and a marked-up manuscript including supplemental figures and an added table. We have addressed all the comments raised by both reviewers, and we believe our manuscript has been improved.

Thank you very much for your consideration.

Sincerely, Hiroki Kashimura et al.

“Shortwave radiative forcing, rapid response, and feedback to the surface by sulphate geoengineering: Analysis of the Geoengineering Model Intercomparison Project G4 scenario” by Hiroki Kashimura et al.

Response to Dr. Aaron Donohoe

Dear Dr. Donohoe

We thank Dr. Donohoe for a careful review again and constructive comments. Please find below the authors’ response. In this reply we denote referee's comments and questions using blue; our responses are in black and relevant text in the manuscript in Times font with changes shown in red.

I want to thank the Author’s for the careful and thoughtful revisions and response to reviews. The revised manuscript is technically sound, well written and has addressed my previous concerns. I believe the conclusions are sound, novel and will make a strong impact on the existing literature on geoengineering. I continue to disagree with the emphasis on the surface energy budget (as opposed to TOA) and think the distinction between shortwave feedbacks and rapid response to SRM could be brought to the forefront of the manuscript in order to reach a broader climate dynamics audience. However, that emphasis is simply my opinion on the importance of the work and, as written, the focus on the changes in net shortwave at the surface is justified within the text. I elaborate on my suggestion below and otherwise have only minor suggestions of clarification. I think this manuscript is publishable nearly as is. Thanks again to the Author’s for their efforts.

Primary emphasis of the text.

The main conclusion I draw from the results presented in this manuscript are: if one accounts for inter-model spread in the adjusted radiative forcing under SRM management, inter-model spread in surface temperature response is primarily due to differences in the shortwave forcing (as opposed to feedbacks). The spread in the adjusted forcing is a consequence of both the inter-model differences in the direct aerosol forcing and the rapid cloud response and the Authors have developed a novel technique for separating the direct forcing and rapid cloud response. The implication of this work is: the climate response to greenhouse gases and SRM can be understood from simply calculating the adjusted forcing and using the same climate sensitivity. While there is work to be done to understand the rapid cloud response – and where the observed system may lie within the substantial inter-model spread – I think this conclusion is a powerful result that I have not seen stated elsewhere. If robust, it would suggest that running long SRM model simulations is less important than understanding the short term cloud response to aerosol. I think this result is significant to the larger climate dynamics community and should be the central focus of the writing in the manuscript.

Again, this is just my opinion. As written, I think the manuscript addresses the more specific issue of how surface shortwave will change under SRM and this may be of more interest to the geo-engineering community that is reading this special issue. I personally think the results and implications are impactful to a larger community. But I leave it to the Authors to make this determination since they know their audience better than I do.

=> Thank you very much for the suggestion. We think it would be very fruitful to write a companion piece talking about understanding the climate response from this sort of 'dual forcing' experiment. So as not to distract from the main point of the present paper, which we would prefer to keep focused on SRM, we reserve such discussions for future work.

Specific points:

Section 3.4:Comparison of feedbacks with those estimated from greenhouse forcing; The Authors find an ensemble average surface albedo feedback of +0.38 W $m^{-2}K^{-1}$ and a shortwave water vapor absorption feedback of -0.91 W $m^{-2}K^{-1}$ at the surface. It would be helpful to compare these feedbacks to those (ensemble average over the larger CMIP5 ensemble) reported in the literature under the response to greenhouse forcing. Numbers for the TOA are more prevalent in the literature and I suggest reporting TOA numbers here too (since the technique used in the manuscript gets at both). Specifically, these numbers seem consistent with the ensemble mean surface albedo feedback at TOA of +0.3W m^{-2} K^{-1} given by Bony et al. feedback review paper (since the surface number should be slightly bigger in magnitude as discussed in the current manuscript) and the shortwave water vapor absorption of +1.0 W $m^{-2}K^{-1}$ in the atmospheric column and 0.3 W $m^{-2}K^{-1}$ at the TOA (implying -0.7 at the surface) given by Donohoe et al. 2014 (Shortwave and longwave contributions to global warming under increasing carbon dioxide, PNAS). I think the point that the SW feedbacks in response to SRM are consistent with those under greenhouse forcing is a powerful statement.

=> Following this suggestion, we have calculated feedback parameters at TOA and compared them with Soden and Held (2006) (which Bony et al referred) and Donohoe et al. (2014). We found that the SW feedback of surface albedo is consistent with those under greenhouse forcing, but that of WV is about a half. This discussion is added at the end of Section 4.1 as follow:
P.14 L.27–35 "To fairly compare feedback parameters in G4 with those under greenhouse gas forcing, we decompose the total reactions at TOA into rapid adjustment and feedback in the same manner that we performed in Section 3.4. The rapid adjustment and feedback parameters calculated at TOA are listed in Table S1. The multi-model-averaged feedback parameter of surface albedo in G4 is 0.27 W m^{-2} K^{-1}. This value is close to the surface albedo feedback parameter of 0.26 W m^{-2} K^{-1} in A1B scenario Soden and Held (2006) and that of 0.30 W m^{-2} K^{-1} in the quadrupled CO_2 experiment Donohoe et al. (2014). On the other hand, the multi-model-averaged feedback parameter of water vapour in G4 is 0.15 W m^{-2} K^{-1} and that (for SW at TOA) in quadrupled CO_2 experiment is 0.30 W m^{-2} K^{-1}. These comparisons suggest that the SW feedback of surface albedo under sulphate geoengineering is consistent with that under greenhouse gas forcing, whereas that of water vapour is about a half of that under greenhouse gas forcing."

Page 14. Line 18. Worth pointing out that the 35% difference between surface albedo feedback as measured at the TOA compared to that at the surface is consistent with the (single pass) basic state atmospheric opacity (1-A-R).

=> Thanks to this comments, we realized that the ratio E_{SA}^{TOA}/E_{SA} can be mathematically written as (1-A-R)/(1-R). And of course, this ratio is consistent with the 35% difference. We added a word and a sentence as follows:
P.14 L.3–5 "This is mainly because the upward shortwave radiation that was reflected at the surface must pass the atmosphere being decreased by absorption and reflection before reaching the TOA. The ratio E_{SA}^{TOA}/E_{SA}, of course, agrees with $(1-R^{as}_{RCP}-A^{as}_{RCP})/(1-R^{as}_{RCP})$, which can be obtained through algebraic manipulation."

Page 14. Line 20. The impact of shortwave atmospheric absorption on reflected SW at the TOA has 2 contributions in response to decreased water vapor under SRM: 1. Less absorption of shortwave above cloud top results in less shortwave reflected off the top of clouds reaching the TOA and 2. Less absorption above bright surfaces reduces the surface contribution to reflected SW at the TOA. The Author's are correct in pointing out that 2 dominates in the isotropic SW model used in this study by construction since the atmospheric absorption and reflection occur at the same vertical level (hence prohibiting the absorption above cloud top. This is a limitation of the model (I'm criticizing myself not the Authors here – Lol). But, in the real world it's possible that the SW water vapor absorption above cloud top is the dominant affect over the surface contribution. I don't know of and can't think of a way to back out the relative contributions, but it's worth discussing this point in the text.

If we understand the referee's point correctly, we should discuss the relative contribution of absorption above the cloud and that above the surface. As the referee mentioned, our single layer model assumes reflection and absorption at the same level and at the same time, and this model cannot consider the order of reflection and absorption. The SW flux that reflected back to TOA by clouds and the atmosphere without reaching the surface is independent on the change of atmospheric absorption rate in this model.
Thanks to this referee's comment, we realized that E_{wv}^{TOA} could be underestimated, and we added a note mentioning about this as follows:
P.14 L.17–20 "Note that, in our single layer model, SW absorption above the clouds is not included, so that upwelling SW at TOA reflected by the clouds without reaching the surface is independent of the absorption rate. Therefore, E_{WV}^{TOA} could be underestimated, and the change in water vapour may not be negligible for the energy budget at TOA."

Page 10. Line 32. Suggest rewording to "... implying that decreases in water vapor and cloud amount under SRM lead to more downwelling SW at the surface, counteracting the enhanced aerosol reflection by SRM".

=> We modified the sentence as suggested.
P.9 L19–20 "Both E_{WV} and E_C are positive, implying that the decreases in water vapour

and cloud amounts under SRM lead to more downwelling SW at the surface, counteracting the enhanced aerosol reflection by SRM."

Page 10. Lines 33-34. The text suggest that decreases in water vapor are due to surface cooling only, where as I would have thought that the robust positive rapid response in Ewv (positive) implies that the atmosphere dries out before the surface cools due to reduced convection as soon as the aerosol is added to the atmosphere. If the specific humidity data are readily available, it would be nice to see if this logic holds (i.e. the direct response to SRM is a reduction in relative humidity).

=> As you pointed out, because the rapid response of E_{WV} is positive, the temperature drop is not the only reason for the water vapour decrease. We modified the sentence as follows:
P.9 L20–21 "One reason for the decrease of water vapour is the temperature reduction, which results in less evaporation (Kravitz et al., 2013)."
Then, we revised sentences in Section 3.4. Please see the next response.
At this time, the specific humidity data is not available for all models, so we reserve such analysis for future work.

Page 12. Line 5. Confusing intro sentence – I think it meant to say no qualitive differences in Ewv. I suggest the following: "WV changes lead to a robust ensemble average increase in surface SW under SRM. This increase in surface SW is due to both the rapid decrease in WV in direct response to SRM (+0.3 W m^{-2}) and the WV decrease due to surface cooling (-0.91 W m^{-2} K^{-1} – note the negative sign corresponds to an increase in surface shortwave with cooling)."

=> To avoid confusion, we revised the related sentences as follows:
P.11 L.24–28 "E_{WV} shows high negative correlation with ΔT in all models, and the rapid adjustment (+0.30 W m^{-2} in multi-model mean) and the feedback (-0.91 W m^{-2} K^{-1}) are clearly separated. That is, the surface SW increase due to less water vapour is caused by both the rapid direct response to SRM and the surface cooling; note that the negative sign corresponds to an increase in surface SW with cooling. The rapid decrease of the water vapour would result from reduced convection due to change in vertical temperature profile caused by the injected stratospheric sulphate aerosols."

NOTE: I think there was a sign error in the manuscript, since the two should have opposite signs if one is cited as a feedback.

=> You are correct. –0.30 should be +0.30.

Page 13. Line 28-29. Is the robust cloud reduction in the Western Pacific part of the feedback or rapid response to SRM? I don't know the literature well enough to evaluate if this spatial pattern is consistent with the cloud response one would expect from the cooling, the rapid adjustment, or is all together different.

=> Because E_C is calculated from the difference between G4 and RCP4.5, all features in E_C are caused by SRM directly or indirectly. The Gregory-plot analysis showed that the rapid response is dominant in E_C (though it varies a lot). Detailed analysis is needed to detect what physical effect is dominant in the Western Pacific, but exploration for a specific region is out of scope of this study.

Section 4.2. This whole section confused me. Shouldn't the impact of stratospheric changes in LW emissivity be evaluated from radiative changes at the tropopause after stratospheric temperature adjustment? The argument presented is instead written in terms of TOA radiative response and I'm not sure the sign of the impact is even the same. Additionally, the second paragraph talks about evaluating the impact of stratospheric LW adjustment from the rapid response where I would have though the LW rapid adjustment would have been dominated by the substantial changes in clouds in the troposphere.

=> We carefully reconsider the role and importance of this section in our manuscript. Then we realized that Section 4.2 provides a little information on LW rapid adjustment of WV but we cannot evaluate its importance compared with SW total reactions and LW feedbacks (which cannot be evaluated easily). We decided to remove this section. We believe keeping focus on SW analysis will benefit readers.

Page 17. First line. I would make this statement stronger – one should expect that the rapid adjustment in response to SRM is very different from that due to CO2 because the vertical distribution of the direct forcing is very different (partitioning of radiative anomalies between the surface and atmospheric column.

=> Thank you for your suggestion. We changed the sentence as follows:
P.16 L7–9 "One should expect that the rapid adjustment in response to SRM is different from that due to CO_2, because the vertical distribution of the direct forcing is different

and the cloud rapid adjustment can be caused by various processes (e.g., changes in atmospheric stability)."

We also corrected the following typos in the manuscript.

- 2070 => 2069 (The SRM term had to be written as year 2020 to 2069 not 2070)
- E^{TOA}_{SA} => E^{TOA}_{WV}, E_{SA} => E_{WV} (P.14 L.17, typo)

“Shortwave radiative forcing, rapid response, and feedback to the surface by sulphate geoengineering: Analysis of the Geoengineering Model Intercomparison Project G4 scenario” by Hiroki Kashimura et al.

Response to the Referee #3

Dear Referee

We thank the referee for a careful review and constructive comments. Please find below the authors’ response. In this reply we denote referee's comments and questions using blue; our responses are in black and relevant text in the manuscript in Times font with changes shown in red.

General Comments:

The paper estimates the shortwave (SW) radiative forcing at the surface from the injection of sulfur in to the stratosphere. Their method is applied to the GeoMIP G4 models where 5 Mt SO_2 is injected annually in a transient RCP4.5 scenario. A single layer model for SW radiative transfer is used to calculate the forcing of the aerosol layer, rapid adjustments and reactions from changes in water vapor, cloud amount, and surface albedo. The simple model is a simplification but it allows to differentiate between different effects and provide useful information relevant to human activities and interests and the assumptions made are clearly stated. The paper will be a valuable addition to current literature on the subject after some minor revisions.

A number of scatter plots are included in the analysis where means over 3 decades are used. These single values should be split into decadal means such that you have three values to base the analysis on instead of one. This will not only provide more data points for the regression, but also indicate more clearly the steadiness of the differences in climates over this period of the simulations.

=> We carefully considered your suggestion. After splitting the 30 year means into three 10-year means, we obtained the following figure (ensemble runs are omitted):

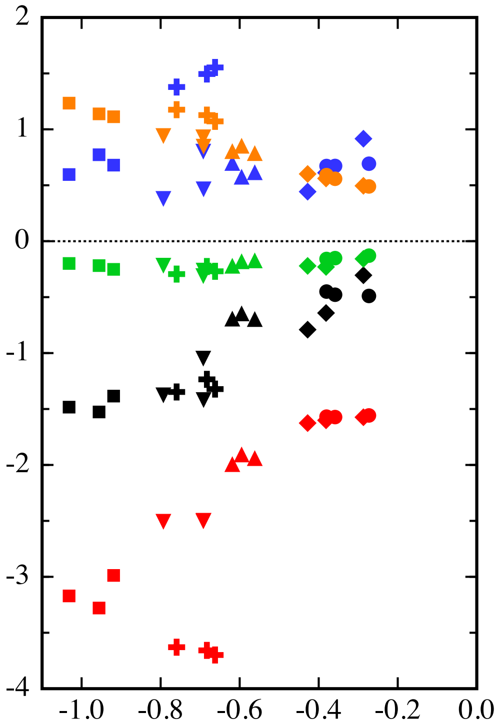

We find that this figure does not add additional information beyond what we obtained from the 30-year mean, and it has the drawback of being substantially busier. Note that, in addition to the above figure, 45 data points for each variable are needed to plot ensemble members (15 runs x 3 decades), which are required in the text. Moreover, the baseline experiment (RCP4.5) is transient, so treating the three different decadal means requires some care. We find the 30-year mean to be simpler. Note that time-dependence/steadiness is shown in Fig. 4.

Throughout the manuscript there is content that belongs only in the figure captions and not in the main text. E.g. “(shown by red symbols)” and similar is unnecessary in the main text; more interesting to read about the meaning of the results in the figures than color coding etc.

=> Following your suggestion, we removed them form the main text. Note that words pointing which Figure to see, E.g., “(Fig. 9b)”, are remained, because they benefit readers to follow the descriptions and discussions.

You should make some concluding remark on what your findings imply for human activities at the surface, as this is your initial motivation for the paper, and put your findings into a wider context.

=> Our biggest finding is that the large range (uncertainty) of SRM forcing in the simulated sulphate geoengineering. So that, we consider it is not the stage to make a direct conclusion for influence on human activities, even it was our initial motivation. Most important thing is to take note this large uncertainty in considering an environmental assessment of the sulphate geoengineering. To mention this, we added the following sentence:
P.15 L.26–27 "From a point of view of an environmental assessment of sulphate geoengineering, we note that there is such large uncertainty in the simulated SRM forcing."

Specific comments:

- The brief 'review' of solar constant experiments p. 2 lines 6-14 is not very informative nor important for this paper. I suggest removing it.
  => We removed almost all of these lines and just remained one sentence with references.

- P2, l19: 'arctic' should be 'Arctic'.
  => We corrected it as suggested.

- P2 l17-26: you mention a number of sulfate aerosol papers, but you do not say how or why they or their findings are relevant or important. Either just list them and say they cannot be compared or find something relevant. Otherwise, it is merely "stuffing".
  => We agree that the sentences were too long and less informative. Here, what we intended to say is "There are many studies but comparison is difficult", so that listing is necessary enough. We revised to list them in a new Table 1 to avoid long sentences.

- P3 l18-32: you discuss factors explaining the spread in the climate response in G4. It would be interesting if you could also note down the spread in the RCP4,5 models (for the same models as in the G4 study referred to) for comparison. Is the spread larger for G4?
  => This comparison was done in the refereed paper (Yu et al. 2015). The spread for RCP4.5 is ±0.21 and G4's spread is larger. We added a sentence

as follows:

P.3 L.15–16 "This spread is larger than that of ± 0.21 K of temperature increase in RCP4.5 scenario for the same models."

- P3 l34: 'behaivour' -> 'behaviour'.

  => We corrected it as suggested.

- P3 l34 and P4 l4, l8: you refer to several, recent and many studies; please include some citations.

  => We added Andrews (2014) and Zhang et al. (2016) for (previous) P3 L34, Trenberth et al (2014) and Wild et al. (2014) for P4 L4, and Campillo et al. (2012) for P4 L8.

- P4 l11: radiation at the surface is also important for oceanic processes like biogeochemistry and ocean carbon cycle. This should be mentioned too. Human activities, like fisheries, might also be affected at sea.

  => Thank you for the suggestion. We added a sentence as follows:

  P.3 L.32–33 "Surface SW is also important for ocean carbon cycle and fisheries through changes in amounts of phytoplankton (Miller et al., 2006)."

- P5 l4: "In addition, the microphysics of the tropospheric sulphate aerosols is not calculated in MIROC-ESM-CHEM-AMP to avoid drift in the simulated climate." Why would this cause a drift? Please note a brief explanation in the text.

  => We modified the sentence and added a brief explanation as follows:

  P.4 L.28–31 "Because the newly developed microphysics module for sulphate aerosols in MIROC-ESM-CHEM-AMP was not well-tested or tuned for the troposphere by a long-term climate simulation yet, it may cause unexpected drift in the simulated climate due to changes in concentration and/or distribution of the tropospheric sulphate aerosols. To avoid such situation, the sulphate aerosol microphysics was calculated only in the stratosphere in G4 and RCP4.5."

- P5 l6: The experiment has also been done with NorESM – and maybe IPSL and MPI-ESM(?). CSIRO-Mk3L has done 'G4S', which is not G4, hence no need to mention.

  => IPSL-CM5A-LR and NorESM1-M performed the experiment but they have some issues in calculation of LW effects of sulphate aerosols as written in Ferraro and Griffiths (2016, ERL). To the best of our knowledge, MPI-ESM did not perform G4. We added the following sentence and removed the sentence on CSIRO-Mk3L.

P.5 L.2–3 "IPSL-CM5A-LR (Dufresne et al., 2013) and NorESM1-M (Bentsen et al., 2013; Iversen et al., 2013) have some issues in calculation of the LW effects of the sulphate aerosols (Ferraro and Griffiths, 2016)".

- P6, l12: 'cloud effects': do you mean feedbacks due to clouds?

  => Here, the word "cloud effects" means effects of cloud on radiative transfer, which is simply defined by all-sky value minus clear-sky value of model outputs (radiative fluxes) and calculated R, A and α. To avoid confusion, we revised the sentence as follows:

  P.6 L.8 "Defining the cloud effects on radiative transfer for a variable X by"

- P7: on what time-scales are these assumptions valid?

  => We consider these assumptions are independent of time-scale, at least up to the period of G4 experiment.

- P7: EC –cloud amount: this can also be output as a variable from the models. Do any of the models account for injected sulfate interactions with clouds? e.g. Kuebbeler et al. ?

  => Some do, and some don't. The strength of the indirect effects in models (at least for models that include such effects) varies considerably, and we didn't want to distract from the main point of the paper by getting into such discussions. We reserve that for future work.

- Figure 2: Why was year 2020 of RCP4.5 used as 'baseline'? Why not center the baseline on a 5 or 10 year period around 2020, to account for variability of the climate considering 2020 might be a particularly warm or cold year. It would be a cleaner comparison, particularly for BNU-ESM who has a lot of year-to-year variability.

  => As suggested, we updated Fig. 2 to use baseline for mean of 5 years (2018-2022).

- P8 l11-12: "For all models, T in G4 decreases or remains at the 2020 level for a few decades and begins increasing from around 2040 or earlier": This is a bit inaccurate. For models a-c, yes, but not really for the MIROC models.

  => The word "2020 level" was used for roughly same (~ ±0.3 K), but as the referee mentioned the range of "level" depends on readers. We revised the sentence as follows:

P.8 L9–10 "For all models, T in G4 decreases or remains within +0.3 K from the baseline for a few decades and begins increasing from around 2040 or earlier, whereas T in RCP4.5 steadily increases."

- Figure 2 discussion; you're applying a fixed magnitude forcing every year, whilst the anthropogenic forcing in RCP4.5 keeps increasing. Hence the limitation to the cooling evolution you describe on page 8. Include some comment on this in the discussion of the results.

  => We included a sentence as follows:

  P.8 L.14–15 "This is simply because the anthropogenic forcing in RCP4.5 keeps increasing but the amount of SO_2 injection per year is fixed in G4."

  Here, we avoid to say "the magnitude of SRM forcing is fixed" at this point (though it is naturally expected), because we are showing that the evolution of SRM forcing in Fig. 4, which is almost constant during the SRM period.

- Why is there hardly any cooling in MIROC-ESM-CHEM?

  => This is what we explored in this study, and the main reason is the weakness of F_{SRM} in MIROC-ESM-CHEM as shown in Fig. 5.

- P8 l 17: " … and then returns to the RCP4.5 level in each model": HadGEM2-ES has not returned to RCP4.5 levels at the end of the run as this model has a larger temperature response to the forcing. You may include the comment that the stronger the temperature response to the forcing is, the longer it takes to return to the otherwise temperature path and the rate of change of the climate system to sudden termination would become more drastic.

  => We had used the word "RCP4.5 level" very roughly and it was inaccurate. We revised this sentence as follow:

  P.8 L.15–16 "In addition, after halting SRM at 2070, T increases rapidly and then returns to or approaches the RCP4.5 level in each model."

  As you commented, it might be true that the stronger temperature cooling by SRM needs longer time to return to RCP4.5 path. However, Fig. 2 is an inter-model comparison, so that model properties (inertia or sensitivity) may also affect the speed of temperature rising. And we cannot distinguish them from our results (at least without many additional analyses). In addition, SRM termination is not focused in this study. From above reasons, we avoid to state something more on temperature rising at SRM termination.

- Figure 3: You find a correlation coefficient of 0.88. Please include the regression line in the figure. Also you select data from three decades as the temperature differences between G4 and RCP4.5 are steady over this period. I suggest you therefore use one value from each decade in every run in the figure. Then you have more data points and information.
  => Regression line was included as suggested.
  As we explained in the response to the referee's "general comments" we decided not to split 30-year mean to three 10-year mean.

- Figure 4: Fsrm varies by ~1 Wm-2 throughout G4 in HadGEM2-ES. Why is this so much more variable than the other model that accounts for formation and transportation of the aerosols (MIROC-ESM-CHEM-AMP)?
  => Both HadGEM2-ES and MIROC-ESM-CHEM-AMP calculate formation and transportation of the sulphate aerosols, but details are different. We explained this in the text as follows:
  P. 4 L.23–31 "In HadGEM2-ES, the tropospheric aerosol scheme and the associated microphysical properties (Bellouin et al., 2011) is simply extended into the stratosphere. Modifications to the stratospheric aerosol size distribution have been applied in subsequent HadGEM2-ES studies (Jones et al., 2016ab), but have not been applied here. In MIROC-ESM-CHEM-AMP, the microphysics module for stratospheric sulphate aerosols treats them in three modes as shown in Table 2 in Sekiya et al. (2016); however, to calculate radiative processes on the aerosols, a particle size of 0.243 um is assumed for simplification. Because the newly developed microphysics module for sulphate aerosols in MIROC-ESM-CHEM-AMP was not well-tested or tuned for the troposphere by a long-term climate simulation yet, it may cause unexpected drift in the simulated climate due to changes in concentration and/or distribution of the tropospheric sulphate aerosols. To avoid such situation, the sulphate aerosol microphysics was calculated only in the stratosphere in G4 and RCP4.5."
  We imagine that such difference in the implementation of sulphate aerosol microphysics may cause the difference in the magnitude of F_{SRM}'s fluctuation. However, at this time, we do not have any evidences or logics that support such imagination. Hence, in the manuscript, we cannot state why this happens.

- Section 3.3: Considering the focus on the last three decades you should break the 3 decade mean into 1 mean for each decade, as mentioned before. The scatter plots have to be updated accordingly.
  => Again, as we explained in the response to the referee's "general comments" we decided not to split 30-year mean to three 10-year mean.

- "HadGEM2-ES does not calculate the sulphate aerosols in the tropospheric and stratosphere: separately" is mentioned several times. Please explain. Not clear what is meant by this at all.
  => In HadGEM2-ES, the sulphate aerosol microphysics module (and its physical parameters) is not tuned for stratosphere. They use the same routine with the same parameters for both troposphere and stratosphere. Accordingly, the output variables related to the sulphate aerosols such as AOD of an air column is the sum of all vertical levels. So that, the available sulphate AOD for HadGEM2-ES is not the AOD for **stratospheric** sulphate aerosols. To make clear this point, we modified the sentence as follows:
  P.10 L11–14 "Note that the above value for HadGEM2-ES is the difference (G4 - RCP4.5) in the sulphate AOD for both troposphere and stratosphere. This is because HadGEM2-ES used the same microphysics calculation of the sulphate aerosols with the same aerosol size distribution in both the troposphere and the stratosphere; sulphate AOD solely for the stratosphere is not available for HadGEM2-ES."

- P10, l23-24: please say "… considered having performed the G4 simulation" – or similar at end of sentence. I.e. point to G4.
  => We modified the sentence as follows:
  P.10 L.21–23 "Pitari et al. (2014) have shown that, in the G4 simulation, SW radiative forcing at the tropopause calculated off-line by a radiative transfer code (Chou and Suarez, 1999; Chou et al., 2001) varies from around 2.1 to 1.0 W m^2 between the models."

- P11, end of section 3.3: can you explain more clearly why the cloud amount is strongly dependent on the initial conditions? To my belief the clouds are even more so dependent on the cloud parameters. (perturbed initial conditions ensembles versus perturbed physical parameter ensembles.)
  => The modeled cloud can be more dependent on the cloud parameters. However, the ensemble runs of MIROC-ESM-CHEM were performed by changing initial condition only, and cloud parameters were same among the

ensemble members. Therefore, we can say that the variety among the ensemble members is due to variations in the initial conditions. We modified the sentence as follows:
P.11 L.11–14 "The variability among the ensemble members implies that the cloud amount is considerably affected by the chaotic properties and high sensitivity to the initial state of the Earth system or ESM, because any model settings other than the initial state are the same among the ensemble members."

- Figure 7: I am not sure how much sense it makes to draw regression lines for Ec. There is clearly little correlation. Also; which models years are included in the figure? 2020 – 2069? Please make a note in caption.
  => I agree that correlation of E_C is very little. However, we consider we should keep the regression line for E_C in the figure for consistency in the information included in the figure.
  The model years of 2021–2070 had been included in the previous manuscript; however, it was inappropriate because the last year of the SRM is 2069. We updated the figure with using 2021-2069. Accordingly, Table 3 was slightly updated. We added the year info in the caption as follows:
  Caption of Fig. 7 "Globally and annually averaged relationship between ΔT and E_{WV} (orange ◇), E_C (blue +), and E_{SA} (green ×) for each year from 2021 to 2069."

- Figure 7 cont.: Have you tried to plot annual means for years 1-10 of the simulations and then decadal means for the remaining 4 decades? This might be more representative for gauging fast vs slow response.
  =>We tried as suggested. However, clarity did not improve, and almost the same results were obtained. Since the clarity did not improve, we keep the figure as before. We consider plotting annual mean is more simple and straightforward.

- Section 3.5 Figure 8: good if you could remind readers at this stage if each model has been weighted by number of ensemble member in these figures.
  => The following note was added to the caption of Fig. 8.
  Caption of Fig. 8 "Note that the multi-model mean is calculated by averaging ensemble means (or single run for models that has no ensembles) of the six models. That is, in the multi-model mean, each run of a model is weighted by the reciprocal of the ensemble number of the model."

- Figure 8 clearly indicates that something is going on with the South Pacific Convergence Zone. Detailed study of this is beyond the topic of your study; however, if this is discussed elsewhere in the literature, it would be great to point to it in the text.
  => We need more detailed analysis to say something meaningful. However, as you mentioned, exploration for a specific region is out of scope of this study. We left it as our future work.

- P13, l25: "However, the situation at TOA is also of interest." Please say why.
  => The reason is simple: the energy budget of the Earth system is closed at TOA. To mention this, we modified the sentence as follows:
  P.13 L.24–25 "However, the situation at TOA is also of interest, because the energy budget of the Earth system is closed at TOA."

- Section 4.2: doesn't the LW heating from the aerosols also increase water vapor in the stratosphere, contributing to ozone losses? This aspect might be mentioned here briefly, as stratospheric O3 amounts do indeed impact human activities at the surface.
  =>The other referee also commented on this section to say this section is confusing. We carefully reconsidered the role and importance of this section in our manuscript. Then we realized that Section 4.2 provides a little information on LW rapid adjustment of WV but we cannot evaluate its importance compared with SW total reactions and LW feedbacks (which is mentioned in your comment and cannot be evaluated easily). We decided to remove this section. We believe keeping focus on SW analysis will benefit readers. Mentioning ozone losses would benefit the reader, so that we added a sentence at the end of text as follows:
  P.17 L1–3 "On the other hand, in the stratosphere, the LW absorption by the injected sulphate aerosols will heat the air and increase water vapour, which contributes to ozone losses (Tilemes et al., 2008; National Research Council, 2015)."

We also corrected the following typos in the manuscript.

- 2070 => 2069 (The SRM term had to be written as year 2020 to 2069 not 2070)
- E^{TOA}_{SA} => E^{TOA}_{WV}, E_{SA} => E_{WV} (P.14 L.17, typo)

Shortwave radiative forcing, rapid adjustment, and feedback to the surface by sulphate geoengineering: Analysis of the Geoengineering Model Intercomparison Project G4 scenario

Hiroki Kashimura[1,a], Manabu Abe[1], Shingo Watanabe[1], Takashi Sekiya[1], Duoying Ji[2], John C. Moore[2], Jason N. S. Cole[3], and Ben Kravitz[4]

[1]Japan Agency for Marine-Earth Science and Technology, Yokohama, Japan.
[2]College of Global Change and Earth System Science, Beijing Normal University, Beijing, China.
[3]Canadian Centre for Climate Modelling and Analysis, Environment and Climate Change Canada, Victoria, British Columbia, Canada.
[4]Atmospheric Sciences and Global Change Division, Pacific Northwest National Laboratory, Washington, USA.
[a]current affiliation: Department of Planetology/Center for Planetary Science, Kobe University, Kobe, Japan.

Correspondence to: Hiroki Kashimura (hiroki@cps-jp.org)

Abstract. This study evaluates the forcing, rapid adjustment, and feedback of net shortwave radiation at the surface in the G4 experiment of the Geoengineering Model Intercomparison Project by analysing outputs from six participating models. G4 involves injection of 5 $\mathrm{Tg\,yr^{-1}}$ of SO_2, a sulphate aerosol precursor, into the lower stratosphere from year 2020 to ~~2070~~ 2069 against a background scenario of RCP4.5. A single layer atmospheric model for shortwave radiative transfer is used to estimate the direct forcing of solar radiation management (SRM), and rapid adjustment and feedbacks from changes in the water vapour amount, cloud amount, and surface albedo (compared with RCP4.5). The analysis shows that the globally and temporally averaged SRM forcing ranges from -3.6 to -1.6 $\mathrm{W\,m^{-2}}$, depending on the model. The sum of the rapid adjustments and feedback effects due to changes in the water vapour and cloud amounts increase the downwelling shortwave radiation at the surface by approximately 0.4 to 1.5 $\mathrm{W\,m^{-2}}$ and hence weaken the effect of SRM by around 50 %. The surface albedo changes decrease the net shortwave radiation at the surface; it is locally strong (~ -4 $\mathrm{W\,m^{-2}}$) in snow and sea ice melting regions, but minor for the global average. The analyses show that the results of the G4 experiment, which simulates sulphate geoengineering, include large inter-model variability both in the direct SRM forcing and the shortwave rapid adjustment from change in the cloud amount, and imply a high uncertainty in modelled processes of sulphate aerosols and clouds.

1 Introduction

Geoengineering, or climate engineering, is the deliberate large-scale manipulation of the planetary environment to counteract anthropogenic climate change (e.g., Shepherd, 2009). One major category of geoengineering for lessening the effects of global warming is solar radiation management (SRM), which aims to reduce the amount of solar radiation at the Earth's surface. One of several SRM approaches (e.g., Lane et al., 2007) is to mimic a volcanic eruption by injecting sulphate aerosol precursors, such as SO_2, into the stratosphere (e.g., Budyko, 1974; Crutzen, 2006); this approach is called sulphate geoengineering. Large volcanic eruptions carry SO_2 gases into the stratosphere; these gases are photo-chemically oxidized to form sulphate aerosols, which have high reflectivity in the visible and ultraviolet regions of the electromagnetic spectrum. Sulphate aerosols increase the solar reflectivity of the atmosphere, decreasing the shortwave radiation (SW) reaching the surface, and therefore cooling the air temperature. For example, the 1991 eruption of Mount Pinatubo reduced the globally averaged surface air temperature by up to 0.5 K (Parker et al., 1996).

To explore the cooling effect of and the climate responses from sulphate geoengineering, or more generally SRM, several climate-modelling groups performed various experiments using global climate models or Earth System Models (ESMs). Some experiments involved simplifying the net effects of SRM by reducing the solar constant ~~. Govindasamy and Caldeira (2000) and Bala et al. (2008) performed a doubling experiment with a 1.8 % reduction of the solar constant, and showed that such a decrease would compensate the global mean temperature change caused by the doubling in their models.Govindasamy et al. (2002) consi the impact of the solar constant reduction on the terrestrial biosphere, whilst a quadrupling experiment with a 3.6 % reduction of the solar constant was explored in Govindasamy et al. (2003). Furthermore, Matthews and Caldeira (2007) adopted the IPCC A2 scenario (IPCC, 2007) as their reference simulation and performed experiments in which the geoengineering was applied for different years. Others~~ (Govindasamy and Caldeira, 2000; Bala et al., 2008; Govindasamy et al., 2002, 2003; Matthews and Caldeira whereas, the studies listed in Table 1 have simulated sulphate geoengineering with models that can partly or fully calculate the production of sulphate aerosols from the injected SO_2 and the dynamical transportation. ~~For example, Rasch et al. (2008a) designed their experiments with injection by 2–4 in an equatorial region with doubled , whereas Robock et al. (2008) adopted the A1B scenario as their baseline run and injected 3–10 of from arctic or tropical regions in their simulation. The models used in these two studies include formation, transportation, and removal of the stratospheric sulphate aerosols, but the particle size distribution was prescribed. Heckendorn et al. (2009) and Pierce et al. (2010) calculated full microphysics of sulphate aerosols with an assumption of zonally homogeneous conditions. They simulated 2–20 injection with a present day (year 2000) condition run as their reference simulation. Niemeier and Timmreck (2015) used models with full microphysics of sulphate aerosols, and performed a sulphate geoengineering experiment with injection rates of 2–200 to counteract the anthropogenic forcing of RCP8.5. Most of the aforementioned studies used different forcing and/or schemes~~ The listed studies used different forcing for geoengineering, different scenarios for the baseline, and different models. Therefore, it is difficult to compare these studies or evaluate the uncertainty in the geoengineering simulations. However, Jones et al. (2010) compared the results of two different models in an experiment similar to that of Robock et al. (2008). They showed the different responses by the two models and emphasized the importance of intercomparing many different climate models with a common experimental design in order to assess the impact of the geoengineering.

The Geoengineering Model Intercomparison Project (GeoMIP) (Kravitz et al., 2011) was established to coordinate simulations with a common framework and to determine the robust effects and responses to geoengineering processes. For the first series of GeoMIP experiments, four experiments named G1, G2, G3, and G4 were proposed. The first two are designed to counteract quadrupled CO_2 radiative forcing (G1) and a 1 % increase in the CO_2 concentration per year (G2) by simply reducing the solar constant. The last two are designed to inject SO_2 into the lower stratosphere and decrease SW flux reaching the surface by increasing the SW reflection by sulphate aerosols. Both G3 and G4 use the RCP4.5 scenario for the baseline experiment and inject SO_2 every year from 2020 to ~~2070.~~ 2069. The amount of SO_2 injected in G3 gradually increases to maintain the net radiative flux at the top-of-atmosphere (TOA) at the 2020 levels, while the radiative forcing of the greenhouse gases increases according to the RCP4.5 scenario. Conversely, in G4 the SO_2 injection rate is fixed at 5 $\mathrm{Tg\,yr^{-1}}$. A summary of the G1–G4 studies is presented by Kravitz et al. (2013d) and the latest list of GeoMIP studies is available at http://climate.envsci.rutgers.edu/GeoMIP/index.html.

As summarized by Kravitz et al. (2013d), studies analysing GeoMIP experiments have explored and clarified climate model responses to radiative forcing and its dependence on various factors. In addition, the dependence (or uncertainty) of the direct forcing to the net surface SW induced by sulphate aerosol injection (hereafter SRM forcing) on models should be also studied well, since estimation of the SRM forcing is important when considering the costs and benefits of geoengineering. The G1 and G2 experimental designs have limited utility in understanding sulphate aerosol geoengineering because the SRM is introduced simply and directly by the reduction of the solar constant. In G3, the amount of injected SO_2 mimicked in each model varies by year, which is useful for controlling the absolute amount of forcing but not the injection rate. In contrast, in G4 the rate of SO_2 injection is fixed at 5 $\mathrm{Tg\,yr^{-1}}$ throughout the SRM period, and the annually averaged strength of the SRM forcing should be almost constant during the SRM period in each model, but may differ among models. Therefore, the G4 experiment is suitable for directly exploring the strength and the model dependence or uncertainty of the SRM forcing.

There are numerous sources of inter-model differences in response to the same (or similar) forcing. On processes related to the SRM forcing, modelled aerosol microphysics including formation, growth, transportation, and removal may differ, and such differences result in the difference in meridional distribution of the aerosol optical depth (AOD). Even though the prescribed AOD is given, a difference in an assumed particle size for the stratospheric sulphate aerosols causes difference in the SRM forcing (Pierce et al., 2010). On a broad scale, different models have distinct climate sensitivities and thus different global mean temperature responses to the same forcing. In addition, different models have various representations of processes, which affects the direct response to the forcing as well as different feedback from the responses. For example, cloud adjustments (Schmidt et al., 2012), sea ice changes (Moore et al., 2014), and stratospheric ozone changes (Pitari et al., 2014) are all known to affect the climate response to geoengineering through feedback. The ocean response operates on longer timescales and has also been shown to be important in understanding the response to geoengineering (Kravitz et al., 2013b). Yu et al. (2015) calculated the difference in globally and temporally averaged near-surface air temperature of G4 (over 2030–2069) from "baseline climate" (RCP4.5 over 2010–2029) and showed a standard deviation of up to ± 0.31 K among models, while the model mean of the temperature difference was 0.28 K. This spread is larger than that of ± 0.21 K of temperature increase in RCP4.5 scenario for the same models. Whilst the models in G4 assume the same rate of SO_2 injection, model responses to the SRM differ widely. Investigation into what causes such a large inter-model variability is very important for SRM simulation studies.

A simple procedure is used for quantifying the contributions of different types of SW rapid adjustments and feedbacks in the climate model ~~behaivour~~ behaviour to geoengineering with stratospheric sulphate aerosols. Here, a rapid adjustment is defined as a reaction to the SRM forcing without changes in globally averaged surface air temperature, whereas a feedback is defined as a reaction due to surface air temperature changes in the global mean induced by the SRM forcing (e.g., Sherwood et al., 2015). (Hereafter, the term "total reaction" refers to the sum of a rapid adjustment and a feedback.) In recent studies of the climate change, rapid adjustments are included in forcing agents and the concept of effective radiative forcing is widely used (e.g., Andrews, 2014; Zhang et al., 2016). However, for the study of the sulphate geoengineering simulation, which is not well verified by observations and thus is expected to have many uncertainties, the separation of the direct forcing and total reactions is important to improve the simulation and to enhance the degree of understanding of the sulphate geoengineering by refining individual related processes. Many studies on climate energy balance have analysed changes in the net radiation flux at TOA, where the energy budget is closed by SW and longwave radiation (LW) (e.g., Trenberth et al., 2014; Wild et al., 2014). However, in the geoengineering study, the radiative changes at the surface are also important, because vegetation, agriculture, and solar power generation for example will be strongly affected by radiative changes at the surface as well as surface temperature changes . (e.g., Campillo et al., 2012). Surface SW is also important for ocean carbon cycle and fisheries through changes in amounts of phytoplankton (e.g., Miller et al., 2006). Though the surface energy budget is balanced among SW, LW, sensible heat flux, and latent heat flux, Kleidon et al. (2015) showed that the latter three are mainly determined by the air and/or surface temperature. Hence, this study focuses on changes in surface air temperature and SW. The direct SW forcing to the surface are evaluated by considering the total reactions due to changes in water vapour amounts, cloud amounts, and surface albedo. Also, these total reactions are decomposed into adjustments and feedbacks, which indicate the rapid change just after injection of SO_2 and the change with globally averaged surface air temperature change by SRM, respectively. We provide results for both global and local effects, focusing on cross-model commonalities and differences. The following section describes the data and methods used in this study. Section 3 presents the results of the analyses. Section 4 provides a short discussion. Summary and concluding remarks are provided in Section 5.

2 Data and methods

The models analysed in this study are listed in Table 2. Note that the method of simulating sulphate aerosols differs among the participating models. HadGEM2-ES and MIROC-ESM-CHEM-AMP calculate the formation of sulphate aerosols from SO_2 injected from the lower stratosphere on the equator, and their horizontal distribution of sulphate AODs differ. BNU-ESM, MIROC-ESM, and MIROC-ESM-CHEM use a prescribed AOD, which is formulated as one fourth of the strength of the 1991 eruption of Mount Pinatubo following Sato et al. (1993) and provided in http://climate.envsci.rutgers.edu/GeoMIP/geomipaod.html. The annual cycle and latitudinal distribution of the prescribed AOD, which is zonally uniform, is shown in Fig. 1; this annual cycle is repeated every year during the SRM period. In CanESM2, a constant field of AOD (~ 0.047) has been given to express the effect of the SO_2 injection. The MIROC-ESM, MIROC-ESM-CHEM, and MIROC-ESM-CHEM-AMP are based on the same framework but differ in their treatment of atmospheric chemistry. An online atmospheric chemistry module is coupled in the MIROC-ESM-CHEM and MIROC-ESM-CHEM-AMP, whereas MIROC-ESM is not coupled with the chemistry module. In the MIROC-ESM-CHEM, the prescribed AOD is used for the stratospheric sulphate aerosols and for the calculation of the surface area density of the sulphur. Conversely, the MIROC-ESM-CHEM-AMP fully calculates the chemistry and micro-physics of the stratospheric sulphate aerosol formation from SO_2 (a detailed description is presented in Sekiya et al., 2016).

The mean stratospheric sulphate aerosol particle sizes and standard deviation of their log-normal distribution (σ) in each model are shown in Table 1. In HadGEM2-ES, the tropospheric aerosol scheme and the associated microphysical properties (Bellouin et al., 2011) is simply extended into the stratosphere. Modifications to the stratospheric aerosol size distribution have been applied in subsequent HadGEM2-ES studies (Jones et al., 2016a, b), but have not been applied here. In MIROC-ESM-CHEM-AMP, the microphysics module for stratospheric sulphate aerosols treats them in three modes as shown in Table 2 in Sekiya et al. (2016); however, to calculate radiative processes on the aerosols, a particle size of 0.243 µm is assumed for simplification. ~~In addition, the microphysics of the tropospheric sulphate aerosols is not calculated~~ Because the newly developed microphysics module for sulphate aerosols in MIROC-ESM-CHEM-AMP ~~to avoid~~ was not well-tested or tuned for the troposphere by a long-term climate simulation yet, it may cause unexpected drift in the simulated climate due to changes in concentration and/or distribution of the tropospheric sulphate aerosols. To avoid such situation, the sulphate aerosol microphysics was calculated only in the stratosphere in G4 and RCP4.5.

Note that the following ~~four~~ five models also participated in the GeoMIP-G4 experiment but are not used in this study. ~~CSIRO Mk3L (Phipps et al., 2011, 2012) mimics the effect of injection by reduction of the solar constant, so the method of analysis described below cannot be used.~~ GEOSCCM (Rienecker et al., 2008) and ULAQ (Pitari et al., 2002) do not include an ocean model and the sea surface temperature is prescribed, so that the surface temperature decrease by the SRM is not simulated in a way that is conducive to the analyses undertaken. IPSL-CM5A-LR (Dufresne et al., 2013) and NorESM1-M (Bentsen et al., 2013; Iversen et al., 2013) have some issues in calculation of the LW effects of the sulphate aerosols (Ferraro and Griffith GISS-E2-R (Schmidt et al., 2006) has issues in its output of clear-sky SW flux at the surface that preclude the incorporation of this data in the analyses.

The model output variables used in this study are monthly means of surface air temperature (T), upwelling and downwelling SW fluxes at the surface and TOA for all-sky and clear-sky. The data for both experiments (RCP4.5 and G4) from the models listed in Table 2 with all ensemble members are used.

Since the SRM forcing is mainly induced by the reflection of the SW by stratospheric sulphate aerosols, the atmospheric reflection rate is very important. In order to consider rapid adjustments and feedbacks on the SW due to the SRM forcing, the atmospheric absorption rate and the surface albedo are also important. To estimate these rates and the albedo from SW fluxes described in the previous paragraph, a single-layer atmospheric model of SW transfer used in Donohoe and Battisti (2011) (hereafter DB11) is applied. DB11's single-layer model assumes that a fraction R of the downwelling solar radiation flux at the TOA S is reflected back to space, and a fraction A is absorbed by the atmosphere at the same single layer. A fraction α of the transmitted radiation flux $S(1-R-A)$ is then reflected by the surface. This reflected upwelling radiative flux is reflected back to the surface at the rate of R and absorbed at the rate of A at the atmospheric layer, and the remainder $S\alpha(1-R-A)^2$ is transmitted to space. This process continues, forming an infinite geometric series, as shown in Fig. 1 of DB11; therefore, the TOA upwelling SW flux ($F^{\uparrow}_{\mathrm{TOA}}$), surface downwelling SW flux ($F^{\downarrow}_{\mathrm{SURF}}$), and surface upwelling SW flux ($F^{\uparrow}_{\mathrm{SURF}}$) can be written as follows:

$$
\begin{aligned}
F^{\uparrow}_{\mathrm{TOA}} &= S\left[R + \alpha(1-R-A)^2 + \alpha^2 R(1-R-A)^2 + \alpha^3 R^2(1-R-A)^2 + \cdots\right] \\
&= SR + \alpha S(1-R-A)^2\left[1 + (\alpha R) + (\alpha R)^2 + \cdots\right] = SR + \alpha S\frac{(1-R-A)^2}{1-\alpha R}, \qquad (1)\\
F^{\downarrow}_{\mathrm{SURF}} &= S\left[(1-R-A) + \alpha R(1-R-A) + \alpha^2 R^2(1-R-A) + \alpha^3 R^3(1-R-A) + \cdots\right] \\
&= S(1-R-A)\left[1 + (\alpha R) + (\alpha R)^2 + (\alpha R)^3 + \cdots\right] = S\frac{(1-R-A)}{1-\alpha R}, \qquad (2)\\
F^{\uparrow}_{\mathrm{SURF}} &= \alpha F^{\downarrow}_{\mathrm{SURF}} = \alpha S\frac{(1-R-A)}{1-\alpha R}. \qquad (3)
\end{aligned}
$$

Here, the infinite series in the second lines of Eqs. (1) and (2) converge to the final expression on the right-hand side because $\alpha R < 1$. The fractions R, A, and α are positive and less than unity. Note that, to the best of our knowledge, the idea of forming the infinite geometric series from SW transfer between a single layer and the surface can be traced back to Rasool and Schneider (1971), who calculated the effect of aerosol on the global temperature by considering a single aerosol layer.

From Eqs. (1)–(3), R, A, and α can be calculated when S, $F^{\uparrow}_{\mathrm{TOA}}$, $F^{\downarrow}_{\mathrm{SURF}}$, and $F^{\uparrow}_{\mathrm{SURF}}$ are given. Surface albedo α can be obtain immediately by Eq. (3) as

$$\alpha = \frac{F^{\uparrow}_{\mathrm{SURF}}}{F^{\downarrow}_{\mathrm{SURF}}}. \qquad (4)$$

Substitution of the product of Eqs. (2) and (3) into Eq. (1) yields

$$R = \frac{SF^{\uparrow}_{\mathrm{TOA}} - F^{\downarrow}_{\mathrm{SURF}}F^{\uparrow}_{\mathrm{SURF}}}{S^2 - F^{\uparrow 2}_{\mathrm{SURF}}}, \qquad (5)$$

for calculating the value of R. Then, A is calculated using values of R and α by the following form of Eq. (2):

$$A = (1-R) - \frac{F^{\downarrow}_{\mathrm{SURF}}}{S}(1-\alpha R). \qquad (6)$$

Note that, R, A, and α cannot be obtained when $S = 0$ such as during the polar night.

Based on the DB11's single-layer model described above, the strength of the SRM forcing and the total reactions due to changes in the water vapour amount, cloud amount, and surface albedo are estimated using the method described in the remainder of this section. Since GeoMIP participating models provide all-sky and clear-sky values for $F^{\uparrow}_{\mathrm{TOA}}$, $F^{\downarrow}_{\mathrm{SURF}}$, and $F^{\uparrow}_{\mathrm{SURF}}$, values of R, A, and α can be calculated for both all-sky and clear-sky; superscript "as" is used for all-sky and "cs" for clear-sky. Defining the cloud effects on radiative transfer for a variable X by $X^{\mathrm{cl}} \equiv X^{\mathrm{as}} - X^{\mathrm{cs}}$, the all-sky value is the sum of the clear-sky value and the cloud effect: $X^{\mathrm{as}} = X^{\mathrm{cs}} + X^{\mathrm{cl}}$, where superscript "cl" is for the cloud effect. For further simplicity, the cloud effect on the surface albedo is assumed to be negligible (i.e., $\alpha^{\mathrm{as}} \approx \alpha^{\mathrm{cs}}$), and α^{as} is used in the following analyses and the superscript omitted. Now, the monthly mean of R^{cs}, R^{cl}, A^{cs}, A^{cl}, and α is calculated on each grid-point for RCP4.5 and G4 experiments.

Net SW at the surface is a key variable in this study and can be written as follows:

$$F^{\mathrm{net}}_{\mathrm{SURF}} \equiv F^{\downarrow\mathrm{as}}_{\mathrm{SURF}} - F^{\uparrow\mathrm{as}}_{\mathrm{SURF}} = (1-\alpha)S\left[\frac{1-(R^{\mathrm{cs}}+R^{\mathrm{cl}})-(A^{\mathrm{cs}}+A^{\mathrm{cl}})}{1-\alpha(R^{\mathrm{cs}}+R^{\mathrm{cl}})}\right]. \qquad (7)$$

Here, $F_{\text{SURF}}^{\text{net}}$ is regarded as a function of S, R^{cs}, R^{cl}, A^{cs}, A^{cl}, and α. The difference of $F_{\text{SURF}}^{\text{net}}$ between RCP4.5 and G4 experiments is defined as

$$\Delta F_{\text{SURF}}^{\text{net}} \equiv F_{\text{SURF}}^{\text{net}}(S, R_{\text{G4}}^{\text{cs}}, R_{\text{G4}}^{\text{cl}}, A_{\text{G4}}^{\text{cs}}, A_{\text{G4}}^{\text{cl}}, \alpha_{\text{G4}}) - F_{\text{SURF}}^{\text{net}}(S, R_{\text{RCP}}^{\text{cs}}, R_{\text{RCP}}^{\text{cl}}, A_{\text{RCP}}^{\text{cs}}, A_{\text{RCP}}^{\text{cl}}, \alpha_{\text{RCP}}), \tag{8}$$

where the experiment names are indicated by subscripts "RCP" and "G4". (S, the TOA downwelling solar radiation, is same for RCP4.5 and G4.) Hereafter, $F_{\text{SURF}}^{\text{net}}(\text{RCP}) \equiv F_{\text{SURF}}^{\text{net}}(S, R_{\text{RCP}}^{\text{cs}}, R_{\text{RCP}}^{\text{cl}}, A_{\text{RCP}}^{\text{cs}}, A_{\text{RCP}}^{\text{cl}}, \alpha_{\text{RCP}})$ is written for convenience.

To estimate the strength of the SRM forcing and the total reactions due to changes in the water vapour amount, cloud amount, and surface albedo on the net SW at the surface, the following is assumed:

1. The sulphate aerosols increased by the SO_2 injection amplify the reflection rate of the clear-sky atmosphere (R^{cs}), whilst their effect on the absorption rate (A^{cs}) is negligible.

2. The change in water vapour amount affects the absorption rate of the clear-sky atmosphere (A^{cs}), whilst its effect on the reflection rate (R^{cs}) is negligible.

3. The amounts of other substances that affects the reflection or absorption rate of the clear-sky atmosphere do not change considerably, and their effects are negligible.

Though the sulphate aerosols can absorb near infrared radiation, which is a part of SW, its effect on the SRM forcing is ignored since its amount is insignificant compared to the SW reflected by the sulphate aerosols (Haywood and Ramaswamy, 1998). (An error due to ignoring the SW absorption by the sulphate aerosols is estimated at the end of this paper.)

Under the above assumptions, the strength of the SRM forcing F_{SRM} is defined by

$$F_{\text{SRM}} \equiv F_{\text{SURF}}^{\text{net}}(S, R_{\text{G4}}^{\text{cs}}, R_{\text{RCP}}^{\text{cl}}, A_{\text{RCP}}^{\text{cs}}, A_{\text{RCP}}^{\text{cl}}, \alpha_{\text{RCP}}) - F_{\text{SURF}}^{\text{net}}(\text{RCP}). \tag{9}$$

This is a change of net surface SW when only R^{cs} is changed to the value of G4. Similarly, the effects of total reactions from changes in the water vapour amount (E_{WV}), cloud amount (E_{C}), and surface albedo (E_{SA}) are defined as follows:

$$E_{\text{WV}} \equiv F_{\text{SURF}}^{\text{net}}(S, R_{\text{RCP}}^{\text{cs}}, R_{\text{RCP}}^{\text{cl}}, A_{\text{G4}}^{\text{cs}}, A_{\text{RCP}}^{\text{cl}}, \alpha_{\text{RCP}}) - F_{\text{SURF}}^{\text{net}}(\text{RCP}), \tag{10}$$

$$E_{\text{C}} \equiv F_{\text{SURF}}^{\text{net}}(S, R_{\text{RCP}}^{\text{cs}}, R_{\text{G4}}^{\text{cl}}, A_{\text{RCP}}^{\text{cs}}, A_{\text{G4}}^{\text{cl}}, \alpha_{\text{RCP}}) - F_{\text{SURF}}^{\text{net}}(\text{RCP}), \tag{11}$$

$$E_{\text{SA}} \equiv F_{\text{SURF}}^{\text{net}}(S, R_{\text{RCP}}^{\text{cs}}, R_{\text{RCP}}^{\text{cl}}, A_{\text{RCP}}^{\text{cs}}, A_{\text{RCP}}^{\text{cl}}, \alpha_{\text{G4}}) - F_{\text{SURF}}^{\text{net}}(\text{RCP}). \tag{12}$$

Here, the following three points should be noted. First, E_{WV}, E_{C}, and E_{SA} are measures for the sum of SW radiative rapid adjustment and feedback, and do not include any LW effects; changes in the water vapour and cloud amounts can, however, affect LW transfer. Second, the sum of F_{SRM}, E_{WV}, E_{C}, and E_{SA} is not exactly equal to $\Delta F_{\text{SURF}}^{\text{net}}$, since Eq. (7) is not linear. However, if $\Delta F_{\text{SURF}}^{\text{net}} \approx F_{\text{SRM}} + E_{\text{WV}} + E_{\text{C}} + E_{\text{SA}}$ is satisfied, it can be stated that the decomposition of $\Delta F_{\text{SURF}}^{\text{net}}$ into F_{SRM}, E_{WV}, E_{C}, and E_{SA} is reasonable. Finally, E_{C} includes both the effect of changes in cloud cover and cloud albedo. This is because R^{cl} and A^{cl} can be written as follows, by expressing R^{as} and A^{as} with the total cloud-area fraction γ, the reflection rate of a fully cloud-covered atmosphere r^{fca}, and the absorption rate of a fully cloud-covered atmosphere a^{fca},

$$R^{\text{cl}} = R^{\text{as}} - R^{\text{cs}} = (1-\gamma)R^{\text{cs}} + \gamma r^{\text{fca}} - R^{\text{cs}} = \gamma(r^{\text{fca}} - R^{\text{cs}}), \tag{13}$$

$$A^{\text{cl}} = A^{\text{as}} - A^{\text{cs}} = (1-\gamma)A^{\text{cs}} + \gamma a^{\text{fca}} - A^{\text{cs}} = \gamma(a^{\text{fca}} - A^{\text{cs}}). \tag{14}$$

These expressions mean that cloud effects (R^{cl} and A^{cl}) include both the total cloud-area fraction and reflection or absorption rate of a fully cloud-covered atmosphere, which depends on cloud albedo or absorption rate. Therefore, E_{C} includes both the effect of changes in coverage, albedo and SW absorption rate of clouds. In addition, E_{C} should not include the "masking effect" (Zhang et al., 1994; Colman, 2003; Soden et al., 2004) of the clouds because the clear-sky values R^{cs} and A^{cs} are unchanged from those in RCP4.5.

In this study, the SRM forcing and the three total reactions on net SW at the surface from the changes in the water vapour amount, cloud amount, and surface albedo, defined by Eqs. (9)–(12), are calculated on each grid-point where $S > 0$ from the monthly mean data. At grid points where $S = 0$, $F_{\text{SRM}} = E_{\text{WV}} = E_{\text{C}} = E_{\text{SA}} = 0$.

To decompose the total reactions (E_{WV}, E_{C}, and E_{SA}) into rapid adjustments and feedbacks, a method similar to the Gregory plot (Gregory et al., 2004) is used. That is, the globally and annually averaged data of total reactions are plotted against that of ΔT ($\equiv T_{\text{G4}} - T_{\text{RCP}}$), and linear regression lines in the following forms are obtained by the least squares method.

$$\overline{E_{\text{WV}}} = Q_{\text{WV}} - P_{\text{WV}}\overline{\Delta T}, \tag{15}$$

$$\overline{E_{\text{C}}} = Q_{\text{C}} - P_{\text{C}}\overline{\Delta T}, \tag{16}$$

$$\overline{E_{\text{SA}}} = Q_{\text{SA}} - P_{\text{SA}}\overline{\Delta T}. \tag{17}$$

Here, Q_X ($X =$WV, C, SA) denotes the rapid adjustment, $-P_X$ is the feedback parameter, and the overline denotes the global and annual average. This method is similar to the Gregory plot, but note that ΔT is the surface temperature difference between the G4 experiment and the RCP4.5 scenario experiment in which the anthropogenic radiative forcing depends on time and the simulated climate does not reach an statistically equilibrium state.

3 Results

3.1 Surface air temperature and shortwave radiation

Figure 2 shows the time series of globally averaged surface air temperature (T) with a 12-month running mean for G4 ~~(solid)~~ and RCP4.5~~(dashed)~~. For all models, T in G4 decreases or remains ~~at the 2020 level~~ within ± 0.3 K from the baseline for a few decades and begins increasing from around 2040 or earlier, whereas T in RCP4.5 steadily increases. Accordingly, the difference in T between RCP4.5 and G4 increases for 10–25 years from 2020 and then stops rising. That is, the cooling effect of SRM gradually affects the global mean of T because of slow feedback and/or thermal inertia of the modelled climate system, and takes a few decades to reach steady state. After that, the SRM becomes unable to prevent the temperature from increasing any more, delaying global warming for a few decades as compared with RCP4.5. This is simply because the anthropogenic forcing in RCP4.5 keeps increasing but the amount of SO_2 injection per year is fixed in G4. In addition, after halting SRM at ~~2070~~the end of 2069, T increases rapidly and then returns to or approaches the RCP4.5 level in each model. This rapid increase has been called the termination effect of SRM (e.g., Wigley, 2006; Jones et al., 2013; Kravitz et al., 2013d).

To properly compare the SRM effects among the models, we eliminate some of the transient behaviour and focus on the years 2040 to 2069, in which the amount of cooling in G4 compared with RCP4.5 is roughly kept constant. (Although the reason for the transient behaviour of the SRM's cooling effect is an important topic, it is beyond the scope of this study.) Figure 3 shows the relationship between ΔT and $\Delta F_{\mathrm{SURF}}^{\mathrm{net}}$, the difference in net SW at the surface, averaged over the globe, for 2040–2069. ~~For CanESM2, HadGEM2-ES, and MIROC-ESM-CHEM, the filled symbols indicate the ensemble mean whilst the unfilled symbols indicate individual ensemble members; for the other models, the filled symbols indicate the results of a single run.~~ This figure shows a strong correlation between the mean ΔT and $\Delta F_{\mathrm{SURF}}^{\mathrm{net}}$; the correlation coefficient for the six filled symbols is 0.88. This strong correlation allows $\Delta F_{\mathrm{SURF}}^{\mathrm{net}}$ to be used as a measure of the SRM effects at least for $-1.1 \lesssim \Delta T \lesssim -0.2$ K, although the surface air temperature depends on the energy balance among SW, LW, and sensible and latent heat fluxes at the surface. Moreover, as described at the end of Section 1, it is important to explore the SW flux at the surface to estimate the effect of SRM on vegetation and human activities such as agriculture and solar power generation. Therefore, this study mainly focuses on SW at the surface and estimates the SRM forcing and total reactions of SW due to changes in the water vapour amount, cloud amount, and surface albedo. One concern is that half the models used in this study have only one ensemble member, and half are MIROC-based models. The effects of this are analysed in Section ~~4.3~~ 4.2 and shown to be relatively unimportant.

3.2 Time-evolution of global mean forcing and SW total reactions

The strength of the SRM forcing (F_{SRM}) defined by Eq. (9) and the SW total reactions due to changes in the water vapour amount (E_{WV}), cloud amount (E_{C}), and surface albedo (E_{SA}) defined by Eqs. (10)–(12) are calculated for each model. Figure 4 shows the time-evolution of the globally averaged values of these measures with a 12-month running mean. $\Delta F_{\mathrm{SURF}}^{\mathrm{net}}$ and ΔT are also shown in this figure. In this subsection, the focus is on the qualitative features common to all or some of the models, whilst the quantitative differences are described in the following subsection.

In the models that used the prescribed or constant AOD field for the SRM (BNU-ESM, CanESM2, MIROC-ESM, and MIROC-ESM-CHEM), F_{SRM} ~~(red)~~ immediately reaches a model-dependent negative value after 2020 and remains almost constant; it then vanishes instantly after the termination. These features are consistent with the fact that the given AOD for the SRM was instantly added and removed in these models. Conversely, in the models that calculate the formation and transport of the sulphate aerosols from the injected SO_2 (HadGEM2-ES and MIROC-ESM-CHEM-AMP), F_{SRM} takes approximately four years to become saturated. During the period in which SRM is imposed, F_{SRM} in MIROC-ESM-CHEM-AMP is almost constant, but F_{SRM} in HadGEM2-ES varies by approximately 1.0 $\mathrm{W\,m^{-2}}$.

The values of E_{SA} ~~shown by the green curves~~ are both negative and small in all of the models. This shows that, at least for the global average, the surface albedo under G4 is higher than that under RCP4.5. However, changes in the surface albedo do not significantly affect $\Delta F_{\mathrm{SURF}}^{\mathrm{net}}$.

Both E_{WV} and E_{C} are positive, implying that the ~~changes in the water vapour amount and cloud amount reduce the amount of the SW decrease~~ decreases in water vapour and cloud amounts under SRM lead to more downwelling SW at the surface, counteracting the enhanced aerosol reflection by SRM. ~~Temperature reduction decreases the amount of evaporation compared with the RCP4.5 scenario and~~ One reason for the decrease of water vapour is the temperature reduction, which results in less ~~water vapour in the atmosphere~~ evaporation (Kravitz et al., 2013c). Less water vapour may cause reduced cloud amounts; less water vapour and reduced cloud amounts increase the atmospheric SW transmissivity and reduce the SRM's cooling effect. The strengths of E_{WV} and E_{C} are comparable in each model except MIROC-ESM-CHEM-AMP (a reason for this exception is discussed in the next subsection). After SRM termination, E_{WV} remains positive for one or two decades. This is consistent with changes in ΔT~~shown by the dashed curves~~; i.e., the water vapour amount in G4 remains less than that in RCP4.5 for a while after the termination. The inter-annual variability of E_{C} is much larger than that of E_{WV}, and the gradual transition to the state of RCP4.5 after the termination (like E_{WV}) is not apparent. Through the whole simulation period, the inter-annual variability of E_{C} dominates that of $\Delta F^{\mathrm{net}}_{\mathrm{SURF}}$. It should be noted that the phases in wave-like, year-to-year variability of $\Delta F^{\mathrm{net}}_{\mathrm{SURF}}$ and ΔT ~~(shown by black solid line and dashed line in Fig. 4)~~ do not agree, although time-averaged $\Delta F^{\mathrm{net}}_{\mathrm{SURF}}$ is well correlated with ΔT as shown in Fig. 3. This is because of thermal inertia and nonlinearities in the Earth system.

3.3 Inter-model dispersion of global mean forcing and SW total reactions

For the inter-model comparison of the results, the global means of F_{SRM}, E_{WV}, E_{C}, and E_{SA} are averaged over the period 2040–2069. Figure 5 shows the relationship between these values ~~(y-axis)~~ and ΔT ~~(x-axis)~~ in the same manner as Fig. 3; $\Delta F^{\mathrm{net}}_{\mathrm{SURF}}$ is shown again. The mean values of F_{SRM} ~~(shown by red symbols)~~ vary widely from approximately -3.6 to $-1.6\ \mathrm{W\,m^{-2}}$, depending on the model. The cooling effect of F_{SRM} in each member or the ensemble mean is reduced by E_{WV} ~~(orange)~~ and E_{C} ~~(blue)~~ and is slightly increased by E_{SA}~~(green)~~. The net effect is approximately equal to $\Delta F^{\mathrm{net}}_{\mathrm{SURF}}$~~(black)~~, which is strongly correlated with ΔT; the residual is less than $0.06\ \mathrm{W\,m^{-2}}$. This supports the validity of the decomposition of $\Delta F^{\mathrm{net}}_{\mathrm{SURF}}$ into SRM forcing and the total reactions due to changes in the water vapour amount, cloud amount, and surface albedo.

The two models with sulphate aerosol calculation (HadGEM2-ES and MIROC-ESM-CHEM-AMP) show stronger F_{SRM} than the others. This outcome indicates that the prescribed AOD, which is based on one-fourth of the Mount Pinatubo eruption, likely underestimates the AOD that results from actual SO_2 injection at a rate of $5\ \mathrm{Tg\,yr^{-1}}$. It is the difference in the mean AOD rather than its meridional distribution as shown in Fig. S1 that leads to the underestimation of the AOD in G4. The globally and temporally averaged stratospheric sulphate AOD in MIROC-ESM-CHEM-AMP is 0.083 and that in HadGEM2-ES is approximately 0.054, though that of the prescribed AOD is 0.037. Note that the above value for HadGEM2-ES is the difference (G4 − RCP4.5) in the sulphate AOD for both troposphere and stratosphere. This is because HadGEM2-ES ~~does not calculate the sulphate aerosols in the tropospheric and stratosphere separately~~used the same microphysics calculation of the sulphate aerosols with the same aerosol size distribution in both the troposphere and the stratosphere; sulphate AOD solely for the stratosphere is not available for HadGEM2-ES.

In CanESM2 and MIROC-ESM-CHEM, the F_{SRM} values are very similar among the ensemble members~~shown by unfilled red symbols~~. This is consistent with the fact that the given AOD fields for mimicking the SO_2 injection effects in G4 are identical among ensemble members of each model. On the other hand, the values of F_{SRM} in the ensemble members of HadGEM2-ES have considerable differences, because the distribution of the sulphate AOD is affected by the chaotic nature of transport and various other processes in the ESM. Even after averaging over 30 years, the mean seasonal cycles of the sulphate AOD can differ among the ensemble members as shown in Fig. S1.

Pitari et al. (2014) have shown that, in the G4 simulation, SW radiative forcing at the tropopause calculated off-line by a radiative transfer code (Chou and Suarez, 1999; Chou et al., 2001) varies from around -2.1 to $-1.0\ \mathrm{W\,m^{-2}}$ between the models. Since both the analysis methods and the participating models presented here differ from those of Pitari et al., it is difficult to compare the two results. However, the results ($F_{\mathrm{SRM}} \sim -3.6$ to $-1.6\ \mathrm{W\,m^{-2}}$) show that model dependence of the SRM forcing might be larger than that shown by Pitari et al.

Figure 5 shows that E_{WV} is strongly anti-correlated with ΔT; the correlation coefficient for the filled symbols is -0.94. In contrast, E_{C} seems to have no correlation with ΔT, with a correlation coefficient of 0.01. This result shows that the SW total reaction from the change in water vapour amount is much simpler (i.e., almost linear with ΔT across all models) than that from changing the cloud amount, which depends strongly on the cloud parameterization scheme. Furthermore, the results of the ensemble members of CanESM2 and MIROC-ESM-CHEM show that the variation in E_{C} mainly causes the variation in $\Delta F^{\mathrm{net}}_{\mathrm{SURF}}$, which is well correlated with ΔT, though F_{SRM} is same among the members. Thus, among the ensemble members, higher E_{C} seems to bring less cooling. MIROC-ESM-CHEM-AMP marks the strongest forcing of the SRM among the models but also marks the largest increase of SW from changing the cloud amount. Accordingly, this model shows the moderate values in $\Delta F^{\mathrm{net}}_{\mathrm{SURF}}$ and ΔT; a possible explanation is given in the following analysis.

To compare ratios of the total reaction and the surface cooling to the magnitude of the SRM forcing, E_{WV}, E_{C}, E_{SA}, and ΔT by $|F_{\mathrm{SRM}}|$ are normalized, as shown in Fig. 6. This figure shows the approximate sensitivity of each total reaction per unit forcing of SRM (y-axis) and the normalized surface cooling(x-axis). The value range of $E_{\mathrm{C}}/|F_{\mathrm{SRM}}|$ (0.19–0.55, blue) is significantly wider than that of $E_{\mathrm{WV}}/|F_{\mathrm{SRM}}|$ (0.27–0.42, orange) and that of $E_{\mathrm{SA}}/|F_{\mathrm{SRM}}|$ (-0.12 to -0.06, green). In addition, the three MIROC-based models show higher $E_{\mathrm{C}}/|F_{\mathrm{SRM}}|$ (0.34–0.55) than other three models (0.19–0.34). This means that the sensitivity of the total reaction due to change in cloud amount in the MIROC-based models is higher than other models. This may be why MIROC-ESM-CHEM-AMP, whose $E_{\mathrm{C}}/|F_{\mathrm{SRM}}|$ is as high as those of MIROC-ESM and MIROC-ESM-CHEM, exhibits high E_{C} and yields moderate cooling, although F_{SRM} is very strong, as shown by the cross sign in Fig. 5. That is, high sensitivity of E_{C} to the SRM forcing will weaken the cooling of surface air temperature as well as $\Delta F^{\mathrm{net}}_{\mathrm{SURF}}$.

The wide variability of $E_{\mathrm{C}}/|F_{\mathrm{SRM}}|$ among the models implies a large uncertainty in the models' cloud processes. Moreover, the spread of $E_{\mathrm{C}}/|F_{\mathrm{SRM}}|$ among nine ensemble members of MIROC-ESM-CHEM is also large. The variability among the ensemble members implies that the cloud amount is considerably affected by the chaotic properties and high sensitivity to the initial state of the Earth system or ESM, because any model settings other than the initial state are the same among the ensemble members. This result therefore suggests that the cooling of the surface air temperature by the SRM depends significantly on the initial state through total reaction due to changes in the cloud amount.

3.4 Decomposition of total reaction into rapid adjustment and feedback

The total reactions due to changes in water vapour amounts, cloud amounts, and surface albedo discussed in the previous two subsections are the sums of the rapid adjustment, which are independent of ΔT, and the feedback, which depends linearly on ΔT. In this subsection, we attempt to decompose the rapid adjustment and the feedback using a so-called Gregory plot (Gregory et al., 2004). Figure 7 shows globally and annually averaged E_{WV}, E_{C}, and E_{SA} as a function of averaged ΔT for each model. Now, we consider that a slope and a y-intercept show a feedback parameter and an amount of rapid adjustment, respectively, as shown by Eqs. (15)–(17); these values and correlation coefficients are shown in Table 3. The multi-model mean values are also shown.

There are no qualitative inter-model differences and each model has the following properties. E_{WV} (orange $\diamond$) shows high negative correlation with ΔT in all models, and the rapid adjustment ($+0.30\ \mathrm{Wm^{-2}}$ in multi-model mean) and the feedback ($-0.91\ \mathrm{Wm^{-2}K^{-1}}$) are clearly separated. In the multi-model mean, the rapid adjustment is -0.30 and the feedback parameter is -0.91 . That is, the surface SW increase due to less water vapour is caused by both the rapid direct response to SRM and the surface cooling; note that the negative sign corresponds to an increase in surface SW with cooling. The rapid decrease of the water vapour would result from reduced convection due to change in vertical temperature profile caused by the injected stratospheric sulphate aerosols.

Unlike E_{WV}, E_{C} (blue $+$) is not well-correlated with ΔT. In addition, the spread of the blue plots E_{C} is large. This means that the rapid adjustment due to cloud changes varies largely, depending on the simulated state of ESM. The feedback of SW cloud radiative effect is not dominant in G4 experiment. Such positive and large rapid adjustment due to the cloud changes and the small cloud feedback are consistent with Kravitz et al. (2013c), who analysed the GeoMIP-G1 experiment.

The y-intercept of E_{SA} (green $\times$) is almost zero, so that the rapid adjustment from the surface albedo change is negligible. The feedback parameter is $0.38\ \mathrm{Wm^{-2}K^{-1}}$ in the multi-model mean, and the strength (absolute value) of the feedback is less than a half of that of E_{WV}.

3.5 Robust features in geographical distribution

To explore robust features in the effects of the SRM in G4, the multi-model mean of the surface air temperature and net SW at the surface is calculated. Figures 8a and 8b show ΔT and $\Delta F_{\mathrm{SURF}}^{\mathrm{net}}$ averaged over the period 2040–2069; hatching indicates regions where 2 or more (out of 6) models disagreed on the sign of the difference. The zonal means are shown in the right-hand side panel for each variable(black indicates the multi-model mean, and coloured lines indicate the ensemble mean of each model). Here, model grid intervals are equal to or narrower than 2.8125 deg, so that the geographical regions mentioned below are represented by enough grid points. However, properties of the Sea of Okhotsk and Hudson Bay may depend on related channels, which may be not well resolved. The geographical distribution of the multi-model mean shows that cooling of the surface air temperature is very strong in and around the Arctic Region, except for Greenland and Europe, and stronger on land than over the ocean in other regions. Such features agree with previous studies such as Robock et al. (2008). Reduction of $F_{\mathrm{SURF}}^{\mathrm{net}}$ is strong in the eastern part of Southern Africa, Tibet, East Asia, Sea of Okhotsk, Hudson Bay, and South America.

In contrast, $F^{\mathrm{net}}_{\mathrm{SURF}}$ increased compared with RCP4.5 in the equatorial region of the Western Pacific, Southern Ocean, except near the Antarctic coast and northern part of the Atlantic. The above reduction and increase are mainly due to E_{C} and E_{SA}; details will be discussed later in this section. The spatial distribution of the sign of $\Delta F^{\mathrm{net}}_{\mathrm{SURF}}$ varies, whereas ΔT is negative over the whole globe. Although ΔT and $\Delta F^{\mathrm{net}}_{\mathrm{SURF}}$ are correlated in the global mean (Fig. 3), the spatial distribution of ΔT does not necessarily need to agree with that of $\Delta F^{\mathrm{net}}_{\mathrm{SURF}}$ because circulation and hydrological processes transport and redistribute energy.

Qualitatively opposite geographical features in ΔT and $\Delta F^{\mathrm{net}}_{\mathrm{SURF}}$ appear in the simulated climate change in RCP4.5 shown in Figs. 8c and 8d, calculated as the difference between the 2010–2039 average and the 2040–2069 average of the RCP4.5 data. Note that the very high positive value in East Asia in Fig. 8d is due to a large reduction of anthropogenic aerosol emission assumed in the late 21st century in the RCP4.5 scenario (Thomson et al., 2011; Westervelt et al., 2015). With the exception of the effects of such assumed emission reduction, sulphate geoengineering can delay global warming almost without regional biases; that is, regions where surface air temperature increases are relatively high in RCP4.5 undergo a large amount of cooling by the sulphate geoengineering and regions with a relatively low increases in temperature receive a small amount of cooling. Model dependence in ΔT shown by coloured lines in Fig. 8a is relatively large in high latitudes in the Northern Hemisphere but small (i.e., comparable with the spread of the global mean ΔT) in other regions. For $\Delta F^{\mathrm{net}}_{\mathrm{SURF}}$ shown in Fig. 8b, all models show qualitatively similar average features at least in the zonal mean, and the range is about $\pm 0.75\ \mathrm{W\,m^{-2}}$.

Next, the multi-model mean of global distributions (averaged over 2040–2069) of (a) F_{SRM}, (b) E_{WV}, (c) E_{C}, and (d) E_{SA} are calculated, as shown in Fig. 9. The SRM forcing is relatively weak in the regions where the annual mean surface albedo is high, such as Greenland, the Sahara, the Middle East, Australia, and Antarctica. This is mainly because the net SW at the surface is low due to the high surface albedo, and accordingly the absolute value of the SRM forcing becomes low. This can be shown via low order approximation: the net SW at the surface can be written as $F^{\mathrm{net}}_{\mathrm{SURF}} \approx (1-\alpha)S(1-R-A)$, and the SRM forcing can be approximated as $F_{\mathrm{SRM}} \approx -(1-\alpha_{\mathrm{RCP}})S(R^{\mathrm{cs}}_{\mathrm{G4}} - R^{\mathrm{cs}}_{\mathrm{RCP}})$, whose absolute value becomes small when α_{RCP} is high. Except for these high surface-albedo regions, the spatial variation in SRM forcing is not very large, even though the incoming solar radiation is strong at low latitudes and weak at high latitudes. This is because the atmospheric reflection rate depends on the solar zenith angle, and the reflection rate becomes higher as the zenith angle increases (e.g., Joseph et al., 1976). That is, strong solar radiation at low latitudes is reflected with low efficiency and weak solar radiation at the high latitudes is reflected with high efficiency. Accordingly, the latitudinal distribution of the SRM forcing is close to uniform in many models. The above feature is a notable aspect in sulphate geoengineering compared with idealized SRM experiments such as G1 and G2, in which the solar constant is simply reduced (Kravitz et al., 2013a) and the forcing is proportional to the cosine of latitude. Latitudinal distribution of F_{SRM} in HadGEM2-ES ~~(purple line in Fig. 9a)~~ and MIROC-ESM-CHEM-AMP ~~(red line in Fig. 9a)~~ shows a stronger latitudinal dependence. These results are consistent with the (approximate) distribution of the stratospheric sulphate AOD as shown in Fig. S1.

The SW total reaction due to the change in the water vapour amount (Fig. 9b) is close to uniform compared with that of the cloud amount (Fig. 9c). The slight increase of E_{WV}, which implies less water vapour, in the equatorial region is consistent of decrease of precipitation reported by Rasch et al. (2008a) and Robock et al. (2008) under SRM. E_{C} has a large spatial variability, which yields many of the spatial variation of $\Delta F^{\text{net}}_{\text{SURF}}$, such as positive values in the equatorial region of the Western Pacific, the Southern Ocean, and the northern part of the Atlantic, and negative values in the eastern part of the Southern Africa, East Asia, and South America. Because $\Delta F^{\text{net}}_{\text{SURF}}$ (Fig. 8b) and the simulated climate change of $F^{\text{net}}_{\text{SURF}}$ in RCP4.5 (Fig. 8d) are opposite in sign, the above result suggests that the SRM offsets increases in the cloud amount simulated in the RCP4.5 scenario, in the positive regions in Fig. 9c and vice versa in the negative regions. The remaining features in $\Delta F^{\text{net}}_{\text{SURF}}$ are caused by the effect of surface albedo change (Fig. 9d), which has large negative values in Tibet, the Sea of Okhotsk, Hudson Bay, and the Southern Ocean near the Antarctic coast. That is, snow and sea ice remain in these regions in the G4 experiment because of the SRM. At high latitudes, the decrease of the net SW at the surface by the change in surface albedo is as large as the SW increase by the change in cloud amount (see the line graph in panels c and d), although E_{SA} is minor in the global mean.

4 Discussion

4.1 Difference between the surface and TOA

This study has focused on the surface net SW because of its importance to human activities. However, the situation at TOA is also of interest, because the energy budget of the Earth system is closed at TOA. Now, we discuss how the measures used in this study differ when TOA is used for the analysis. The net SW at TOA can be written as

$$F^{\text{net}}_{\text{TOA}} \equiv S - F^{\uparrow\text{as}}_{\text{TOA}} = S\left\{1 - (R^{\text{cs}} + R^{\text{cl}}) - \alpha\frac{\left[1 - (R^{\text{cs}} + R^{\text{cl}}) - (A^{\text{cs}} + A^{\text{cl}})\right]^2}{1 - \alpha(R^{\text{cs}} + R^{\text{cl}})}\right\}, \tag{18}$$

so that the direct forcing of SRM and the total reactions measured at TOA ($F^{\text{TOA}}_{\text{SRM}}$, $E^{\text{TOA}}_{\text{WV}}$, $E^{\text{TOA}}_{\text{C}}$, and $E^{\text{TOA}}_{\text{SA}}$) can be calculated in the same manner described in Section 2. Figure 10 shows their globally and temporally averaged values' dependencies on ΔT. The difference of $F^{\text{net}}_{\text{TOA}}$ is also plotted.

The qualitative features of the measures other than $E^{\text{TOA}}_{\text{WV}}$ are same as the analysis at the surface shown in Fig. 6. The quantitative difference in the SRM forcing ($F^{\text{TOA}}_{\text{SRM}} - F_{\text{SRM}}$) is as small as $-0.047\ \text{Wm}^{-2}$ (1.8 %) for the multi-model mean. In contrast, $|E^{\text{TOA}}_{\text{SA}}|$ is less than that of $|E_{\text{SA}}|$ by about 35 %. This is mainly because the upward shortwave radiation that was reflected at the surface must pass the atmosphere being decreased by absorption and reflection before reaching the TOA. The ratio $E^{\text{TOA}}_{\text{SA}}/E_{\text{SA}}$, of course, agrees with $(1 - R^{\text{as}}_{\text{RCP}} - A^{\text{as}}_{\text{RCP}})/(1 - R^{\text{as}}_{\text{RCP}})$, which can be obtained through algebraic manipulation. The difference of $E^{\text{TOA}}_{\text{C}} - E_{\text{C}}$ is $0.12\ \text{Wm}^{-2}$ (16.5 %) for the multi-model mean. Remember that the effect of the cloud amount change includes both changes in reflection rate (R^{cl}) and absorption rate (A^{cl}). The effect of a change in R^{cl} should appear almost equally at the surface and TOA, as the case for the SRM forcing, because both R^{cl} and R^{cs} appear in the Eqs. (7) and (18) in the same way. Therefore, most of $E^{\text{TOA}}_{\text{C}} - E_{\text{C}}$ should be caused by the difference in how the change of the absorption rate affects the net SW at the surface and that at TOA. This is discussed below.

The total reaction at TOA due to the change in water vapour amount shows a negative sign, which is opposite to that at the surface. This disagreement is attributed as follows: Surface cooling reduces the amount of water vapour in the atmosphere and the SW absorption rate decreases. Then, more incoming solar radiation reaches the surface, so that the decrease in water vapour amount increases SW flux at the surface. On the other hand, when the SW absorption rate decreases, the more upwelling SW that was reflected at the surface pass through the atmosphere and reaches TOA. This leads to a cooling effect. Because the effect of decrease in the SW absorption rate is carried to TOA by the upwelling SW that was reflected at the surface by the rate of α, ~~$|E_{\mathrm{SA}}^{\mathrm{TOA}}|$ it~~ $|E_{\mathrm{WV}}^{\mathrm{TOA}}|$ is much less than ~~$|E_{\mathrm{SA}}|$. This does not mean that the~~ $|E_{\mathrm{WV}}|$. Note that, in our single layer model, SW absorption above the clouds is not included, so that upwelling SW at TOA reflected by the clouds without reaching the surface is independent of the absorption rate. Therefore, $E_{\mathrm{WV}}^{\mathrm{TOA}}$ could be underestimated, and the change in water vapour ~~is~~ may not be negligible for the energy budget at TOA~~, because~~. Furthermore, we have not explored LW in this study. An analysis on LW rapid adjustment ~~of clear-sky is discussed in the next subsection, but that of clouds and LW feedback~~ and feedbacks due to changes in water vapour and clouds is left as our future work.

From the above discussion, we have found that the effect of changes in atmospheric SW absorption rate appears differently between at the surface and at TOA (in its sign and amount), but that in reflection rate appears almost equally. The effect of change in the surface albedo is weaker at TOA than at the surface. We will bear these properties in our mind, when we discuss the influence of SRM on the energy budget of the climate system, which is usually considered at TOA, and human activities, which are mainly performed at the surface.

To fairly compare feedback parameters in G4 with those under greenhouse gas forcing, we decompose the total reactions at TOA into rapid adjustment and feedback in the same manner that we performed in Section 3.4. The rapid adjustment and feedback parameters calculated at TOA are listed in Table S1. The multi-model-averaged feedback parameter of surface albedo in G4 is 0.27 $\mathrm{Wm^{-2}K^{-1}}$. This value is close to the surface albedo feedback parameter of 0.26 $\mathrm{Wm^{-2}K^{-1}}$ in A1B scenario (Soden and Held, 2006) and that of 0.30 $\mathrm{Wm^{-2}K^{-1}}$ in the quadrupled $\mathrm{CO_2}$ experiment (Donohoe et al., 2014). On the other hand, the multi-model-averaged feedback parameter of water vapour in G4 is 0.15 $\mathrm{Wm^{-2}K^{-1}}$ and that (for SW at TOA) in quadrupled $\mathrm{CO_2}$ experiment is 0.30 $\mathrm{Wm^{-2}K^{-1}}$. These comparisons suggest that the SW feedback of surface albedo under sulphate geoengineering is consistent with that under greenhouse gas forcing, whereas that of water vapour is about a half of that under greenhouse gas forcing.

4.2 ~~Rapid adjustment of longwave radiation~~

~~This study has concentrated on SW for the reasons described in Section 1; however, it may be valuable for some readers to mention the role of LW. A well-known effect of LW in sulphate aerosol geoengineering is heating of the stratosphere. The sulphate aerosols induced by the injection absorb LW and heat air in the lower the stratosphere (e.g., Heckendorn et al., 2009; Pitari et al. For the energy budget at TOA , increase of the LW absorption results in decrease of the outgoing LW, which manifests as a heating of the climate system. Needless to say, there are many interactions among LW, temperature, and various other components of the climate system through the emission and absorption of LW. Because of such complexity, unlike the SW changes that we have explored in this study, it is difficult to distinguish and estimate the effect of each factor on LW changes.~~

~~One possible and useful analysis for LW is to estimate the rapid adjustment (or response), which is independent of ΔT, by the same method used in Section 3.4. Gregory-like plots are made for the difference of net LW for clear-sky at the surface ($\Delta \mathrm{LW}_{\mathrm{SURF}}^{\mathrm{cs}}$) and at TOA ($\Delta \mathrm{LW}_{\mathrm{TOA}}^{\mathrm{cs}}$) as shown by black "+" signs and red "×" signs, respectively, in Fig. **??**. The rapid~~

adjustment in the clear-sky at the TOA shown by the y-intercept of ΔLW^{cs}_{TOA} regression line shows a heating effect of about 0.57 in the multi-model mean. This rapid adjustment should mainly consist of the effect of LW absorption due to stratospheric sulphate aerosols, since the decrease of the water vapour suggested by the rapid adjustment of E_{WV} yields less LW absorption and an increase in outgoing LW at TOA(i.e., sense of cooling) . It is important to take this heating effect in mind when we consider the energy budget at TOA for sulphate geoengineering. Though the sulphate aerosols' LW effect is significant at TOA, such effect may be less significant at the surface, because the rapid adjustment estimated from ΔLW^{cs}_{SURF} is small compared to the SRM forcingand total reactions at the surface

4.2 Inequality in the number of ensemble and participating models

One concern in this study is that half of the models used have only one ensemble member, and half are MIROC-based models. Because the numbers of ensemble members differ among models as listed in Table 2, each member in each model is not equally weighted in calculation of the multi-model means described in Section 3.5. Responses to the SRM forcing in the three MIROC-based models should be similar to each other as shown in Fig. 6, so that the results of multi-model mean can be biased to that of the MIROC-based models. Therefore, we re-calculated multi-model means by using only one run for each model (Fig. S2); and also tested multi-model means with a weight of 1/3 for the MIROC-based models (Fig. S3). There are no significant difference among Figs. 9, S2, and S3. Therefore, inequality in the number of ensemble and participating models has no significant effects on our results.

5 Summary and concluding remarks

The results from six models (listed in Table 2) that simulated GeoMIP experiment G4, which is designed to simulate sulphate geoengineering by injecting 5 Tg of SO_2 into the stratosphere every year from 2020 to 2070 2069 in the RCP4.5 scenario as the baseline, have been analysed. A single-layer model proposed by Donohoe and Battisti (2011) has been applied to estimate the strength and its inter-model variability of the SRM forcing (F_{SRM}) to the surface net shortwave radiation, whose difference between G4 and RCP4.5 (ΔF^{net}_{SURF}) has a strong correlation with the cooling of the surface air temperature (ΔT), as shown in Fig. 3. The SW total reactions due to changes in the water vapour amount (E_{WV}), cloud amount (E_C), and surface albedo (E_{SA}) have been also estimated. Here, a total reaction is defined as a sum of a rapid adjustment, which does not depend on ΔT, and a feedback, which is proportional to ΔT. Decomposition of the estimated total reactions into the rapid adjustment and the feedback is also done by using a method based on the Gregory plot (Gregory et al., 2004). Note that, unlike the usual Gregory plot, ΔT is defined by the difference between T_{G4} and T_{RCP}, and both experiments are not approaching a statistically equilibrium state, so that the rapid response could vary depending on the state of the modelled climate system.

It has been shown that the globally and temporally averaged F_{SRM} of each model varies widely from about -3.6 to -1.6 $W\,m^{-2}$ (red symbols in Fig. 5).. Inter-model variations comprise a substantial range, and narrowing this uncertainty is essential for understanding the effects of sulphate geoengineering and its interactions with chemical, micro-physical, dynamical, and radiative processes related to the formation, distribution, and shortwave-reflectance of the sulphate aerosols introduced from the SO_2 injection (Rasch et al., 2008b; Kremser et al., 2016). From a point of view of an environmental assessment of sulphate geoengineering, we note that there is such large uncertainty in the simulated SRM forcing.

Our analysis has also shown that, in the global average, changes in the water vapour and cloud amounts (from RCP4.5) increase the SW at the surface and reduce the effect of F_{SRM} by approximately 0.4–1.2 $\mathrm{W\,m^{-2}}$ and 0.5–1.5 $\mathrm{W\,m^{-2}}$, respectively. This is due to the smaller amounts of water vapour and clouds, which mainly block the downwelling solar radiation from reaching the surface by absorption and reflection, respectively. E_{WV} is well correlated with ΔT in multi-model comparison, whereas E_{C} is not. The reduction rate of E_{C} varies from 19 % to 55 % as compared to F_{SRM} depending on both models and ensemble runs (i.e., initial states), whereas that of E_{WV} is 27–42 %. The effect of surface albedo changes is small in the global average, but is significant in the regions where snow or ice melts in the RCP4.5 scenario.

The decomposition analysis has revealed that about 37 % (multi-model mean) of E_{WV} is explained by the rapid adjustment and the rest is the feedback. On the other hand, almost all of E_{C} consists of the rapid adjustment, and a linear relationship between E_{C} and ΔT for the global and annual mean was not obtained for any models. The cloud rapid adjustment in G4 deduced in this study is similar as found for G1 by Kravitz et al. (2013c) but disagree with that in the ~~4xCO2~~ quadrupled CO_2 experiment shown by Andrews et al. (2012). ~~Because~~ One should expect that the rapid adjustment ~~due to changes in clouds~~ in response to SRM is different from that due to CO_2, because the vertical distribution of the direct forcing is different and the cloud rapid adjustment can be caused by various processes (e.g., changes in atmospheric stability)~~, it is possible that the cloud rapid adjustment differs between SRM and global warming~~. More detailed studies on cloud processes in SRM are required for the reduction of the uncertainty and for a better assessment of impact of the sulphate geoengineering on climate and human activities.

The multi-model mean horizontal distribution of ΔT suggests that stratospheric sulphate aerosol geoengineering can delay global warming without significant regional biases, unlike the results of the GeoMIP-G1 experiment (Kravitz et al., 2013a). In G1, the incoming solar radiation was just reduced by a constant fraction, so that the SRM forcing has large latitudinal variation (strong in low-latitudes and weak in high-latitudes). Conversely, in G4, the distribution of sulphate aerosol optical depth (AOD) is internally calculated or externally given, and the reflection of the solar radiation is locally calculated. Here, at least for the prescribed AOD calculated from observed AOD after the 1991 Mount Pinatubo eruption, sulphate aerosols are assumed to spread out globally and form a somewhat uniform distribution as shown in Fig. 1. Because the reflection rate, as well as the incoming solar radiation, depends on the solar zenith angle, as described previously, the resultant SRM forcing does not have large latitudinal variation, as shown in Fig. 9a.

This study has the following three limitations. First, the single-layer model used treats the reflection of downward radiation and that of upward radiation by the same rate. As noted above, however, the reflection rate depends on the incident angle, so errors could be significant in regions that have high solar zenith angle and high surface albedo, such as Greenland and Antarctica.

Second, the SW absorption by the sulphate aerosols has been ignored, because its amount is considered minor compared to the SW reflection. If the absorption by the sulphate aerosols is non-negligible, E_{WV} should be regarded as the sum of a part of SRM forcing by absorption and total reaction due to the change in the water vapour amount, and the forcing and total reaction are not well separated from each other. At least for MIROC-ESM-CHEM, this study confirms that the influence of SW absorption by the sulphate aerosols on E_{WV} is less than 4.5 % by performing the G4 experiment with vanishing SW absorption coefficients of the sulphate aerosols. In other words, the SRM forcing due to SW absorption by the sulphate aerosols is less than 1.5 % of that due to reflection (F_{SRM}). The magnitude of errors in the other models should be similar to that in MIROC-ESM-CHEM.

Finally, SW at the surface has been the focus of this analysis and the energy balance has not been considered. ΔT can be affected by other types of rapid adjustment and feedback. For example, the reduced water vapour in G4 causes less SW absorption by the atmosphere and cooling of the troposphere. The greenhouse effect due to the water vapour would be also decreased. Then, in total, the effect of change in water vapour amount may be a cooling effect (i.e., a positive feedback). However, further On the other hand, in the stratosphere, the LW absorption by the injected sulphate aerosols will heat the air and increase water vapour, which contributes to ozone losses (Tilmes et al., 2008; National Research Council, 2015). Further analysis is required to separate the effect of water vapour from the LW flux. Analyses of the full energy balance and other types of feedback will form part of future work.

6 Data availability

All data used in this study, except for the data of MIROC-ESM-CHEM-AMP, are available through the Earth System Grid Federation (ESGF) Network (http://esgf.llnl.gov). The data of MIROC-ESM-CHEM-AMP are available by contacting the corresponding author.

Author contributions. HK, MA, SW, and TS analysed the data. SW, TS, DJ, JM, and JC developed the models and performed the experiment. BK designed and organized the experiment. All authors contributed to the discussion.

The authors declare that they have no conflict of interest.

Acknowledgements. We thank Dr. Aaron Donohoe and an anonymous reviewer anonymous reviewers for useful comments, which greatly help us to improve the manuscript. We thank all participants of the Geoengineering Model Intercomparison Project and their model development teams, CLIVAR/WCRP Working Group on Coupled Modelling for endorsing GeoMIP, and the scientists managing the Earth System Grid data nodes who have assisted with making GeoMIP output available. We thank Drs. Charles Curry, James M. Haywood, and Andy Jones for model development and comments on the manuscript. We also thank Drs. Masahiro Sugiyama, Hideo Shiogama, and Seita Emori for useful comments. HK, MA, and SW were supported by the SOUSEI Program, MEXT, Japan. Simulations of MIROC-based models were conducted using the Earth Simulator. The Pacific Northwest National Laboratory is operated for the U.S. Department of Energy by Battelle Memorial Institute under contract DE-AC05-76RL01830.

References

Andrews, T.: Using an AGCM to Diagnose Historical Effective Radiative Forcing and Mechanisms of Recent Decadal Climate Change, J. Climate, 27, 1193–1209, 2014.

Andrews, T., Gregory, J. M., Webb, M. J., and Taylor, K. E.: Forcing, feedbacks and climate sensitivity in CMIP5 coupled atmosphere-ocean climate models, Geophys. Res. Lett., 39, L09 712, 2012.

Arora, V. K. and Boer, G. J.: Uncertainties in the 20th century carbon budget associated with land use change, Glob. Change Biol., 16, 3327–3348, 2010.

Arora, V. K., Scinocca, J. F., Boer, G. J., Christian, J. R., Denman, K. L., Flato, G. M., Kharin, V. V., Lee, W. G., and Merryfield, W. J.: Carbon emission limits required to satisfy future representative concentration pathways of greenhouse gases, Geophys. Res. Lett., 38, L05805, 2011.

Bala, G., Duffy, P. B., and Taylor, K. E.: Impact of geoengineering schemes on the global hydrological cycle., P. Natl. Acad. Sci. USA, 105, 7664–7669, 2008.

Bellouin, N., Rae, J., Jones, A., Johnson, C., Haywood, J., and Boucher, O.: Aerosol forcing in the Climate Model Intercomparison Project (CMIP5) simulations by HadGEM2-ES and the role of ammonium nitrate, J. Geophys. Res., 116, D20 206, 2011.

Bentsen, M., Bethke, I., Debernard, J. B., Iversen, T., Kirkevåg, A., Seland, Ø., Drange, H., Roelandt, C., Seierstad, I. A., Hoose, C., and Kristjánsson, J. E.: The Norwegian Earth System Model, NorESM1-M – Part 1: Description and basic evaluation of the physical climate, Geosci. Model Dev., 6, 687–720, 2013.

Budyko, M. I.: Climate and life, Academic Press, New York, 1974.

Campillo, C., Fortes, R., and del Henar Prieto, M.: Solar Radiation Effect on Crop Production, in: Solar Radiation, InTech, 2012.

Chou, M. D. and Suarez, M. J.: A solar radiation parameterization for atmospheric studies, Tech. Rep. TM-1999-104606, NASA Goddard Space Flight Center, Greenbelt, MD, 1999.

Chou, M.-D., Suarez, M. J., Liang, X.-Z., Yan, M. M. H., and Cote, C.: A thermal infrared radiation parameterization for atmospheric studies, Tech. Rep. TM-2001-104606, NASA Goddard Space Flight Center, Greenbelt, MD, 2001.

Collins, W. J., Bellouin, N., Doutriaux-Boucher, M., Gedney, N., Halloran, P., Hinton, T., Hughes, J., Jones, C. D., Joshi, M., Liddicoat, S., Martin, G., O'Connor, F., Rae, J., Senior, C., Sitch, S., Totterdell, I., Wiltshire, A., and Woodward, S.: Development and evaluation of an Earth-System model – HadGEM2, Geosci. Model Dev., 4, 1051–1075, 2011.

Colman, R.: A comparison of climate feedbacks in general circulation models, Clim. Dynam., 20, 865–873, 2003.

Crutzen, P. J.: Albedo enhancement by stratospheric sulfur injections: A contribution to resolve a policy dilemma?, Climatic Change, 77, 211–220, 2006.

Donohoe, A. and Battisti, D. S.: Atmospheric and surface contributions to planetary albedo, J. Climate, 24, 4402–4418, 2011.

Donohoe, A., Armour, K. C., Pendergrass, A. G., and Battisti, D. S.: Shortwave and longwave radiative contributions to global warming under increasing CO_2., Proc. Natl. Acad. Sci. U.S.A., 111, 16 700–16 705, 2014.

Dufresne, J. L., Foujols, M. A., Denvil, S., Caubel, A., Marti, O., Aumont, O., Balkanski, Y., Bekki, S., Bellenger, H., Benshila, R., Bony, S., Bopp, L., Braconnot, P., Brockmann, P., Cadule, P., Cheruy, F., Codron, F., Cozic, A., Cugnet, D., de Noblet, N., Duvel, J. P., Ethé, C., Fairhead, L., Fichefet, T., Flavoni, S., Friedlingstein, P., Grandpeix, J. Y., Guez, L., Guilyardi, E., Hauglustaine, D., Hourdin, F., Idelkadi, A., Ghattas, J., Joussaume, S., Kageyama, M., Krinner, G., Labetoulle, S., Lahellec, A., Lefebvre, M. P., Lefevre, F., Levy, C., Li, Z. X., Lloyd, J., Lott, F., Madec, G., Mancip, M., Marchand, M., Masson, S., Meurdesoif, Y., Mignot, J., Musat, I., Parouty, S., Polcher, J., Rio, C., Schulz, M., Swingedouw, D., Szopa, S., Talandier, C., Terray, P., Viovy, N., and Vuichard, N.: Climate change projections using the IPSL-CM5 Earth System Model: from CMIP3 to CMIP5, Climate Dynamics, 40, 2123–2165, 2013.

Ferraro, A. J. and Griffiths, H. G.: Quantifying the temperature-independent effect of stratospheric aerosol geoengineering on global-mean precipitation in a multi-model ensemble, Environ. Res. Lett., 11, 034 012, 2016.

Govindasamy, B. and Caldeira, K.: Geoengineering Earth's radiation balance to mitigate CO_2-induced climate change, Geophys. Res. Lett., 27, 2141–2144, 2000.

Govindasamy, B., Thompson, S., Duffy, P. B., Caldeira, K., and Delire, C.: Impact of geoengineering schemes on the terrestrial biosphere, Geophys. Res. Lett., 29, 2002.

Govindasamy, B., Caldeira, K., and Duffy, P. B.: Geoengineering Earth's radiation balance to mitigate climate change from a quadrupling of CO_2, Global Planet. Change, 37, 157–168, 2003.

Gregory, J. M., Ingram, W. J., Palmer, M. A., Jones, G. S., Stott, P. A., Thorpe, R. B., Lowe, J. A., Johns, T. C., and Williams, K. D.: A new method for diagnosing radiative forcing and climate sensitivity, Geophys. Res. Lett., 31, L03 205, 2004.

Haywood, J. M. and Ramaswamy, V.: Global sensitivity studies of the direct radiative forcing due to anthropogenic sulfate and black carbon aerosols, J. Geophys. Res., 103, 6043–6058, 1998.

Heckendorn, P., Weisenstein, D., Fueglistaler, S., Luo, B. P., Rozanov, E., Schraner, M., Thomason, L. W., and Peter, T.: The impact of geoengineering aerosols on stratospheric temperature and ozone, Environ. Res. Lett., 4, 045 108, 2009.

IPCC: Climate Change 2007: Synthesis Report, Contribution of working groups I, II and III to the Fourth Assessment Report of the Intergovernmental Panel on Climate Change, IPCC, Geneva, 2007.

Iversen, T., Bentsen, M., Bethke, I., Debernard, J. B., Kirkevåg, A., Seland, Ø., Drange, H., Kristjánsson, J. E., Medhaug, I., Sand, M., and Seierstad, I. A.: The Norwegian Earth System Model, NorESM1-M – Part 2: Climate response and scenario projections, Geosci. Model Dev., 6, 389–415, 2013.

Ji, D., Wang, L., Feng, J., Wu, Q., Cheng, H., Zhang, Q., Yang, J., Dong, W., Dai, Y., Gong, D., Zhang, R. H., Wang, X., Liu, J., Moore, J. C., Chen, D., and Zhou, M.: Description and basic evaluation of Beijing Normal University Earth System Model (BNU-ESM) version 1, Geosci. Model Dev., 7, 2039–2064, 2014.

Jones, A., Haywood, J., Boucher, O., Kravitz, B., and Robock, A.: Geoengineering by stratospheric SO_2 injection: results from the Met Office HadGEM2 climate model and comparison with the Goddard Institute for Space Studies ModelE, Atmos. Chem. Phys., 10, 5999–6006, 2010.

Jones, A., Haywood, J. M., Alterskjær, K., Boucher, O., Cole, J. N. S., Curry, C. L., Irvine, P. J., Ji, D., Kravitz, B., Egill Kristjánsson, J., Moore, J. C., Niemeier, U., Robock, A., Schmidt, H., Singh, B., Tilmes, S., Watanabe, S., and Yoon, J. H.: The impact of abrupt suspension of solar radiation management (termination effect) in experiment G2 of the Geoengineering Model Intercomparison Project (GeoMIP), J. Geophys. Res.-Atmos., 118, 9743–9752, 2013.

Jones, A. C., Haywood, J. M., and Jones, A.: Climatic impacts of stratospheric geoengineering with sulfate, black carbon and titania injection, Atmos. Chem. Phys., 16, 2843–2862, 2016a.

Jones, A. C., Haywood, J. M., Jones, A., and Aquila, V.: Sensitivity of volcanic aerosol dispersion to meteorological conditions: A Pinatubo case study, J. Geophys. Res.-Atmos., 121, 6892–6908, 2016b.

Joseph, J. H., Wiscombe, W. J., and Weinman, J. A.: The delta-Eddington approximation for radiative flux transfer, J. Atmos. Sci., 33, 2452–2459, 1976.

Kleidon, A., Kravitz, B., and Renner, M.: The hydrological sensitivity to global warming and solar geoengineering derived from thermodynamic constraints, Geophys. Res. Lett., 42, 138–144, 2015.

Kravitz, B., Robock, A., Boucher, O., Schmidt, H., Taylor, K. E., Stenchikov, G., and Schulz, M.: The Geoengineering Model Intercomparison Project (GeoMIP), Atmos. Sci. Lett., 12, 162–167, 2011.

Kravitz, B., Caldeira, K., Boucher, O., Robock, A., Rasch, P. J., Alterskjær, K., Karam, D. B., Cole, J. N. S., Curry, C. L., Haywood, J. M., Irvine, P. J., Ji, D., Jones, A., Kristjánsson, J. E., Lunt, D. J., Moore, J. C., Niemeier, U., Schmidt, H., Schulz, M., Singh, B., Tilmes, S., Watanabe, S., Yang, S., and Yoon, J. H.: Climate model response from the Geoengineering Model Intercomparison Project (GeoMIP), J. Geophys. Res.-Atmos., 118, 8320–8332, 2013a.

Kravitz, B., Forster, P. M., Jones, A., Robock, A., Alterskjær, K., Boucher, O., Jenkins, A. K. L., Korhonen, H., Kristjánsson, J. E., Muri, H., Niemeier, U., Partanen, A.-I., Rasch, P. J., Wang, H., and Watanabe, S.: Sea spray geoengineering experiments in the geoengineering model intercomparison project (GeoMIP): Experimental design and preliminary results, J. Geophys. Res.-Atmos., 118, 11,175–11,186, 2013b.

Kravitz, B., Rasch, P. J., Forster, P. M., Andrews, T., Cole, J. N. S., Irvine, P. J., Ji, D., Kristjánsson, J. E., Moore, J. C., Muri, H., Niemeier, U., Robock, A., Singh, B., Tilmes, S., Watanabe, S., and Yoon, J. H.: An energetic perspective on hydrological cycle changes in the Geoengineering Model Intercomparison Project, J. Geophys. Res.-Atmos., 118, 13,087–13,102, 2013c.

Kravitz, B., Robock, A., Forster, P. M., Haywood, J. M., Lawrence, M. G., and Schmidt, H.: An overview of the Geoengineering Model Intercomparison Project (GeoMIP), J. Geophys. Res.-Atmos., 118, 13,103–13,107, 2013d.

Kremser, S., Thomason, L. W., Hobe, M., Hermann, M., Deshler, T., Timmreck, C., Toohey, M., Stenke, A., Schwarz, J. P., Weigel, R., Fueglistaler, S., Prata, F. J., Vernier, J. P., Schlager, H., Barnes, J. E., Antuña Marrero, J. C., Fairlie, D., Palm, M., Mahieu, E., Notholt, J., Rex, M., Bingen, C., Vanhellemont, F., Bourassa, A., Plane, J. M. C., Klocke, D., Carn, S. A., Clarisse, L., Trickl, T., Neely, R., James, A. D., Rieger, L., Wilson, J. C., and Meland, B.: Stratospheric aerosol—Observations, processes, and impact on climate, Rev. Geophys., 54, 278–335, 2016.

Lane, L., Caldeira, K., Chatfield, R., and Langhoff, S., eds.: Workshop report on managing solar radiation, 2007.

Matthews, H. D. and Caldeira, K.: Transient climate–carbon simulations of planetary geoengineering, P. Natl. Acad. Sci. USA, 104, 9949–9954, 2007.

Miller, A. J., Gabric, A. J., Moisan, J. R., Chai, F., Neilson, D. J., Pierce, D. W., and Di Lorenzo, E.: Global change and oceanic primary productivity: Effects of ocean-atmosphere-biological feedbacks, pp. 29–65, no. 73 in Elsevier oceanography series, Elsevier, Amsterdam; Boston, 2006.

Moore, J. C., Rinke, A., Yu, X., Ji, D., Cui, X., Li, Y., Alterskjær, K., Kristjánsson, J. E., Muri, H., Boucher, O., Huneeus, N., Kravitz, B., Robock, A., Niemeier, U., Schulz, M., Tilmes, S., Watanabe, S., and Yang, S.: Arctic sea ice and atmospheric circulation under the GeoMIP G1 scenario, J. Geophys. Res.-Atmos., 119, 567–583, 2014.

National Research Council: Climate Intervention: Reflecting Sunlight to Cool Earth, Reflecting Sunlight to Cool Earth, National Academies Press, Washington, D.C., 2015.

Niemeier, U. and Timmreck, C.: What is the limit of climate engineering by stratospheric injection of SO_2?, Atmospheric Chemistry and Physics, 15, 9129–9141, 2015.

Parker, D. E., Wilson, H., Jones, P. D., Christy, J. R., and Folland, C. K.: The impact of mount Pinatubo on world-wide temperatures, Int. J. Climatol., 16, 487–497, 1996.

Phipps, S. J., Rotstayn, L. D., Gordon, H. B., Roberts, J. L., Hirst, A. C., and Budd, W. F.: The CSIRO Mk3L climate system model version 1.0 – Part 1: Description and evaluation, Geosci. Model Dev., 4, 483–509, 2011.

Phipps, S. J., Rotstayn, L. D., Gordon, H. B., Roberts, J. L., Hirst, A. C., and Budd, W. F.: The CSIRO Mk3L climate system model version 1.0 – Part 2: Response to external forcings, Geosci. Model Dev., 5, 649–682, 2012.

Pierce, J. R., Weisenstein, D. K., Heckendorn, P., Peter, T., and Keith, D. W.: Efficient formation of stratospheric aerosol for climate engineering by emission of condensible vapor from aircraft, Geophys. Res. Lett., 37, L18 805, 2010.

Pitari, G., Mancini, E., Rizi, V., and Shindell, D. T.: Impact of future climate and emission changes on stratospheric aerosols and ozone, J. Atmos. Sci., 59, 414–440, 2002.

Pitari, G., Aquila, V., Kravitz, B., Robock, A., Watanabe, S., Cionni, I., Luca, N. D., Genova, G. D., Mancini, E., and Tilmes, S.: Stratospheric ozone response to sulfate geoengineering: Results from the Geoengineering Model Intercomparison Project (GeoMIP), J. Geophys. Res.-Atmos., 119, 2629–2653, 2014.

Rasch, P. J., Crutzen, P. J., and Coleman, D. B.: Exploring the geoengineering of climate using stratospheric sulfate aerosols: The role of particle size, Geophys. Res. Lett., 35, L02809, 2008a.

Rasch, P. J., Tilmes, S., Turco, R. P., Robock, A., Oman, L., Chen, C.-C., Stenchikov, G. L., and Garcia, R. R.: An overview of geoengineering of climate using stratospheric sulphate aerosols, Phil. Trans. R. Soc. A, 366, 4007–4037, 2008b.

Rasool, S. I. and Schneider, S. H.: Atmospheric carbon dioxide and aerosols: Effects of large increases on global climate, Science, 173, 138–141, 1971.

Rienecker, M. M., Suarez, M. J., Todling, R., Bacmeister, J., Takacs, L., Liu, H. C., Gu, W., Sienkiewicz, M., Koster, R. D., Gelaro, R., Stajner, I., and Nielsen, J. E.: The GEOS-5 data assimilation system-documentation of versions 5.0.1, 5.1.0, and 5.2.0, Technical Report Series on Global Modeling and Data Assimilation, 27, 2008.

Robock, A., Oman, L., and Stenchikov, G. L.: Regional climate responses to geoengineering with tropical and Arctic SO_2 injections, J. Geophys. Res., 113, D16101, 2008.

Sato, M., Hansen, J. E., and McCormick, M. P.: Stratospheric aerosol optical depths, 1850–1990, J. Geophys. Res., 98, 22 987–22 994, 1993.

Schmidt, G. A., Ruedy, R., Hansen, J. E., Aleinov, I., Bell, N., Bauer, M., Bauer, S., Cairns, B., Canuto, V., Cheng, Y., Del Genio, A., Faluvegi, G., Friend, A. D., Hall, T. M., Hu, Y., Kelley, M., Kiang, N. Y., Koch, D., Lacis, A. A., Lerner, J., Lo, K. K., Miller, R. L., Nazarenko, L., Oinas, V., Perlwitz, J., Perlwitz, J., Rind, D., Romanou, A., Russell, G. L., Sato, M., Shindell, D. T., Stone, P. H., Sun, S., Tausnev, N., Thresher, D., and Yao, M.-S.: Present-day atmospheric simulations using GISS ModelE: Comparison to in situ, satellite, and reanalysis data, J. Climate, 19, 153–192, 2006.

Schmidt, H., Alterskjær, K., Bou Karam, D., Boucher, O., Jones, A., Kristjánsson, J. E., Niemeier, U., Schulz, M., Aaheim, A., Benduhn, F., Lawrence, M., and Timmreck, C.: Solar irradiance reduction to counteract radiative forcing from a quadrupling of CO_2: climate responses simulated by four earth system models, Earth Syst. Dynam., 3, 63–78, 2012.

Sekiya, T., Sudo, K., and Nagai, T.: Evolution of stratospheric sulfate aerosol from the 1991 Pinatubo eruption: Roles of aerosol microphysical processes, J. Geophys. Res.-Atmos., 2016.

Shepherd, J. G.: Geoengineering the climate: science, governance and uncertainty, Royal Society, 2009.

Sherwood, S. C., Bony, S., Boucher, O., Bretherton, C., Forster, P. M., Gregory, J. M., and Stevens, B.: Adjustments in the Forcing-Feedback Framework for Understanding Climate Change, Bull. Amer. Meteorol. Soc., 96, 217–228, 2015.

Soden, B. J. and Held, I. M.: An Assessment of Climate Feedbacks in Coupled Ocean–Atmosphere Models, J. Climate, 19, 3354–3360, 2006.

Soden, B. J., Broccoli, A. J., and Hemler, R. S.: On the use of cloud forcing to estimate cloud feedback, J. Climate, 17, 3661–3665, 2004.

Thomson, A. M., Calvin, K. V., Smith, S. J., Kyle, G. P., Volke, A., Patel, P., Delgado-Arias, S., Bond-Lamberty, B., Wise, M. A., Clarke, L. E., and Edmonds, J. A.: RCP4.5: a pathway for stabilization of radiative forcing by 2100, Climatic Change, 109, 77–94, 2011.

Tilmes, S., Müller, R., Salawitch, R. J., Schmidt, U., Webster, C. R., Oelhaf, H., Camy-Peyret, C. C., and Russell III, J. M.: Chemical ozone loss in the Arctic winter 1991–1992, Atmos. Chem. Phys., 8, 1897–1910, 2008.

Trenberth, K. E., Fasullo, J. T., and Balmaseda, M. A.: Earth's Energy Imbalance, J. Climate, 27, 3129–3144, 2014.

Watanabe, S., Hajima, T., Sudo, K., Nagashima, T., Takemura, T., Okajima, H., Nozawa, T., Kawase, H., Abe, M., Yokohata, T., Ise, T., Sato, H., Kato, E., Takata, K., Emori, S., and Kawamiya, M.: MIROC-ESM 2010: model description and basic results of CMIP5-20c3m experiments, Geosci. Model Dev., 4, 845–872, 2011.

Westervelt, D. M., Horowitz, L. W., Naik, V., Golaz, J. C., and Mauzerall, D. L.: Radiative forcing and climate response to projected 21st century aerosol decreases, Atmos. Chem. Phys., 15, 12 681–12 703, 2015.

Wigley, T. M. L.: A combined mitigation/geoengineering approach to climate stabilization, Science, 314, 452–454, 2006.

Wild, M., Folini, D., Hakuba, M. Z., Schär, C., Seneviratne, S. I., Kato, S., Rutan, D., Ammann, C., Wood, E. F., and König-Langlo, G.: The energy balance over land and oceans: an assessment based on direct observations and CMIP5 climate models, Climate Dynamics, 44, 3393–3429, 2014.

Yu, X., Moore, J. C., Cui, X., Rinke, A., Ji, D., Kravitz, B., and Yoon, J. H.: Impacts, effectiveness and regional inequalities of the GeoMIP G1 to G4 solar radiation management scenarios, Global Planet. Change, 129, 10–22, 2015.

Zhang, H., Zhao, S., Wang, Z., Zhang, X., and Song, L.: The updated effective radiative forcing of major anthropogenic aerosols and their effects on global climate at present and in the future, Int. J. Climatol., 36, 4029–4044, 2016.

Zhang, M. H., Hack, J. J., Kiehl, J. T., and Cess, R. D.: Diagnostic study of climate feedback processes in atmospheric general circulation models, J. Geophys. Res., 99, 5525–5537, 1994.

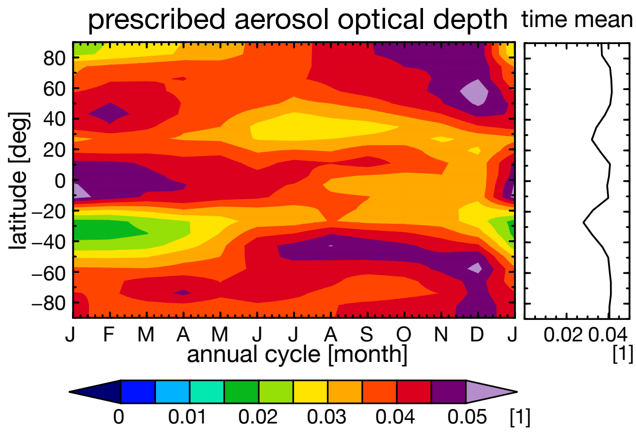

Figure 1. Annual cycle and latitudinal distribution of the prescribed aerosol optical depth provided from the GeoMIP for G4 experiment and used in BNU-ESM, MIROC-ESM, and MIROC-ESM-CHEM. Line graph shows the annual mean.

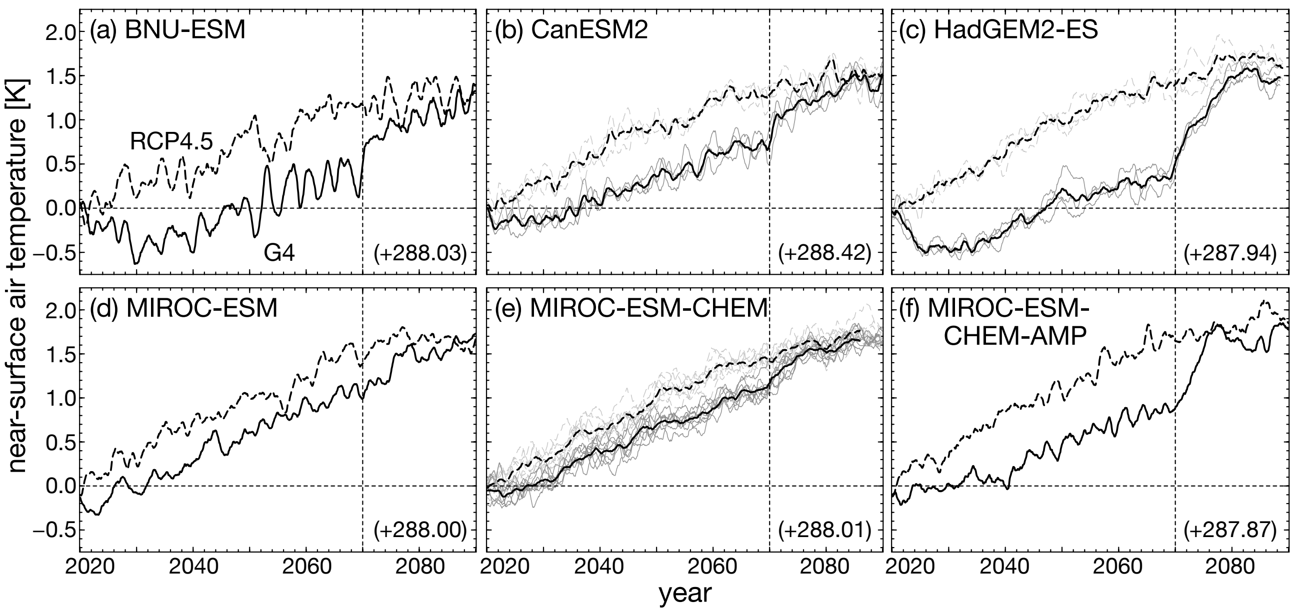

Figure 2. Globally averaged surface air temperature in G4 (solid) and RCP4.5 (dashed) experiments. 12-month running mean is applied. Values are offset by the ~~value at 2020~~RCP4.5 average from 2018 to 2022, the beginning of SRM, shown at the right bottom on each panel. In panels (b), (c), and (e), black curves show the ensemble mean and grey curves show ensemble members. The vertical dashed lines indicate the SRM termination (2070).

~~Same as Fig. 7 but for changes in net LW for clear-sky at the surface (black +) and that at TOA (red ×).~~

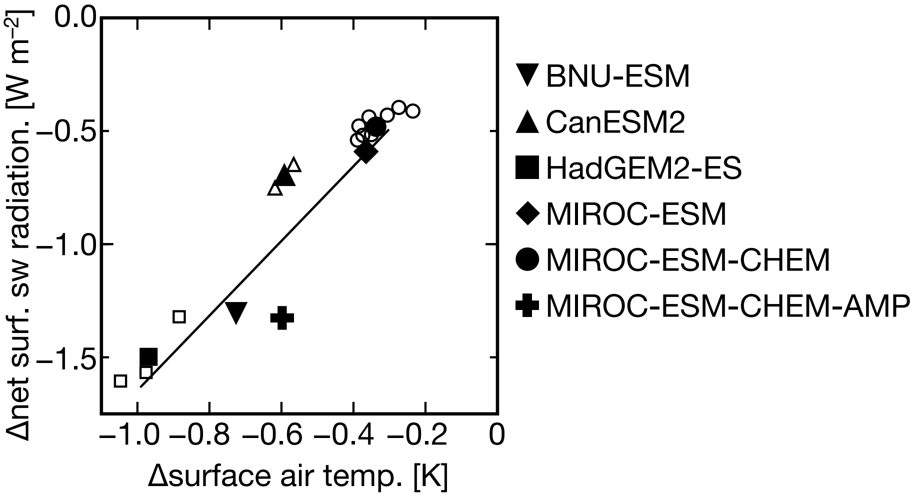

Figure 3. Relationship between the difference in the globally and temporally averaged surface air temperature (x-axis) and that of the net shortwave radiation at the surface (y-axis). The term of average is from 2040 to 2069. For CanESM2, HadGEM2-ES, and MIROC-ESM-CHEM, the ensemble mean is shown by filled symbols and the each member by unfilled ones. The regression line is for the filled symbols of the six models.

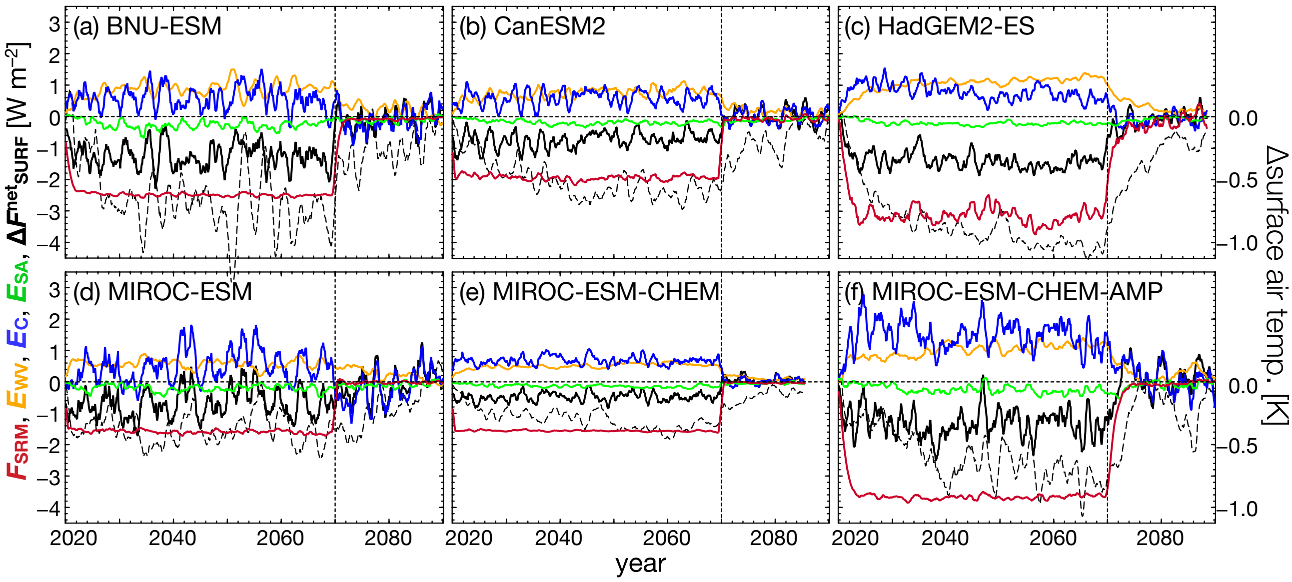

Figure 4. Same as Fig. 2 but for the SRM forcing (red), SW feedback due to changes in the water vapour (orange), cloud amounts (blue), and surface albedo (green) defined in Eqs. (9–12), and the difference in the net shortwave radiation at the surface (black, solid). The difference in the surface air temperature is also plotted by dashed-black curves whose values are shown by the right axis.

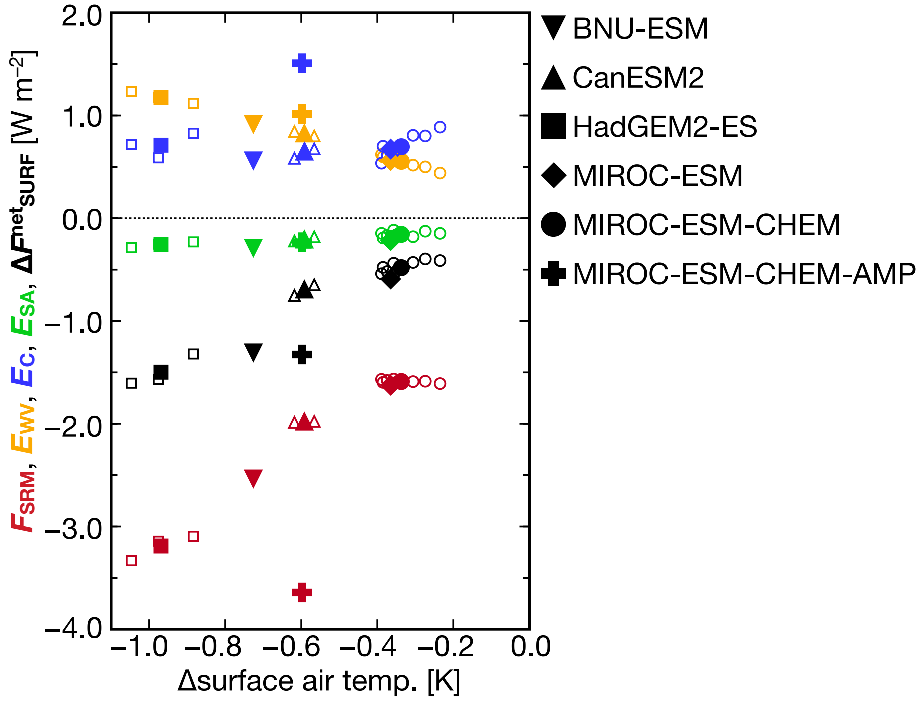

Figure 5. Same as Fig. 3 but also for SRM forcing (red), SW feedback due to changes in the water vapour amount (orange), cloud amount (blue), and surface albedo (green).

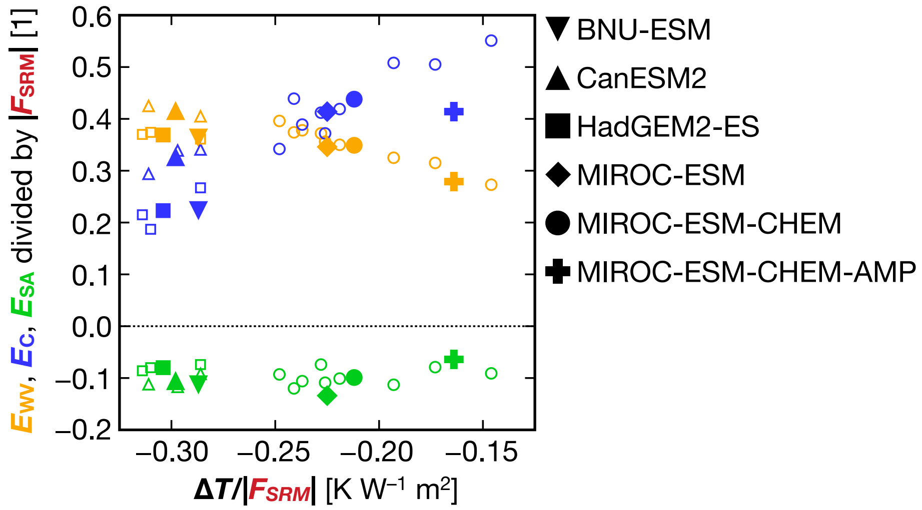

Figure 6. Same as Fig. 5 but for the SW feedback effects normalized by the absolute value of the SRM forcing. Note that the difference in the surface air temperature (x-axis) is also divided by $|F_{\mathrm{SRM}}|$.

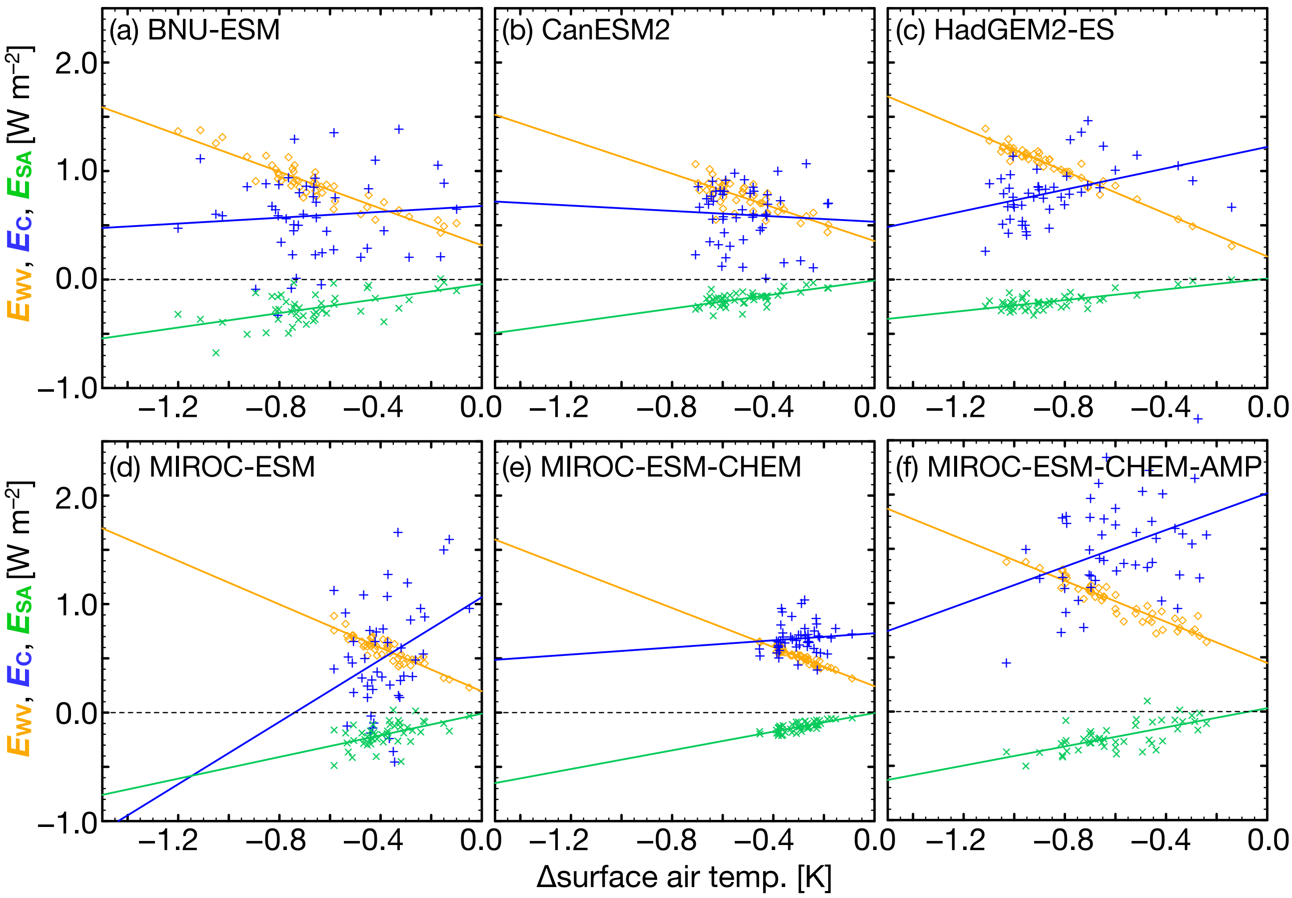

Figure 7. Globally and annually averaged relationship between ΔT (x-axis) and $E_{\rm WV}$ (orange $\diamond$), $E_{\rm C}$ (blue $+$), and $E_{\rm SA}$ (green $\times$) for each year . from 2021 to 2069. Regression line for each plot is shown by the same color, and a slope (feedback parameter), a y-intercept (rapid adjustment), and a correlation coefficient for each plot are shown in Table 3. Ensemble mean data are used for the plots on (b) CanESM2, (c) HadGEM2-ES, and (e) MIROC-ESM-CHEM.

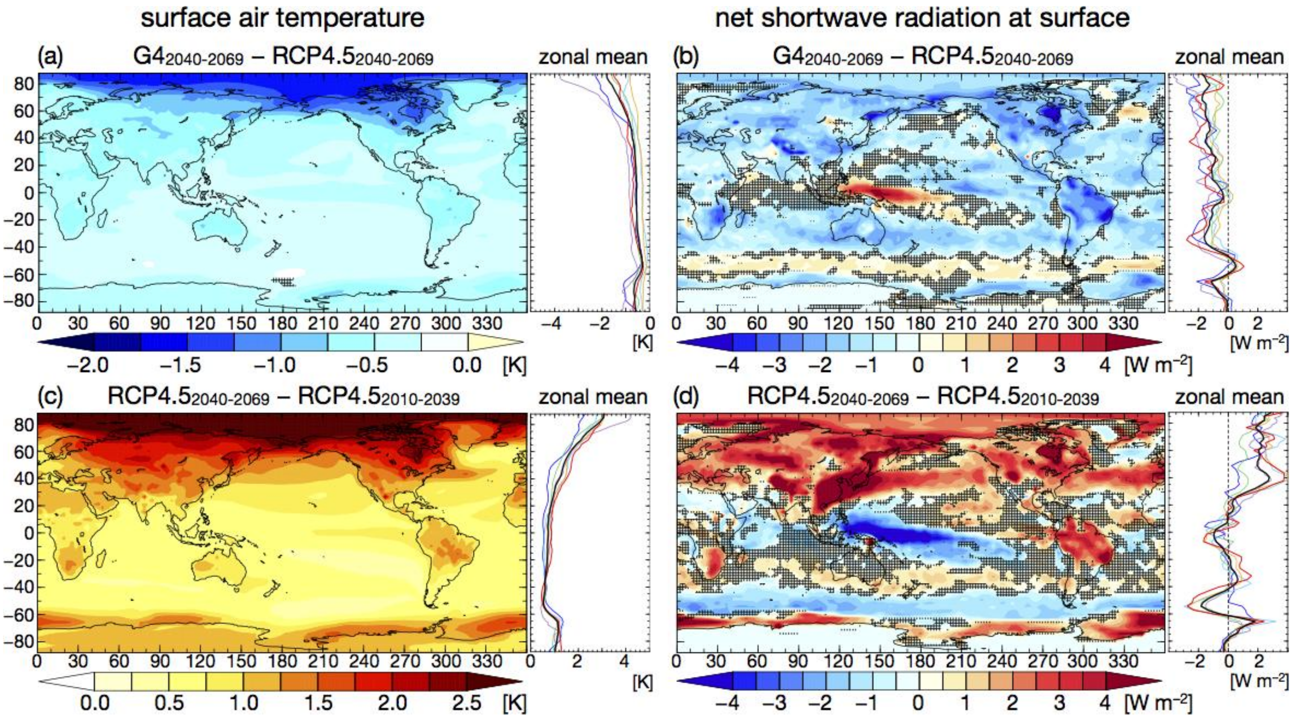

Figure 8. Multi-model mean of difference in the surface air temperature and net shortwave radiation at the surface. Panels (a) and (b) show the difference between G4 and RCP4.5 averaged over 2040–2069. Panels (c) and (d) show the difference between RCP4.5 averaged over 2040–2069 and that over 2010–2039. The colour shading shows the horizontal distribution of the multi-model mean and the black thick line on the right-hand side shows the zonal mean of the multi-model mean. Other coloured thin lines display the ensemble mean (or the result of the single run) of each model (blue: BNU-ESM, green: CanESM2, purple: HadGEM2-ES, cyan: MIROC-ESM, orange: MIROC-ESM-CHEM, red: MIROC-ESM-CHEM-AMP). Hatching indicates the region where 2 or more models (out of 6) disagreed on the sign of the difference. Note that the multi-model mean is calculated by averaging ensemble means (or single run for models that has no ensembles) of the six models. That is, in the multi-model mean, each run of a model is weighted by the reciprocal of the ensemble number of the model.

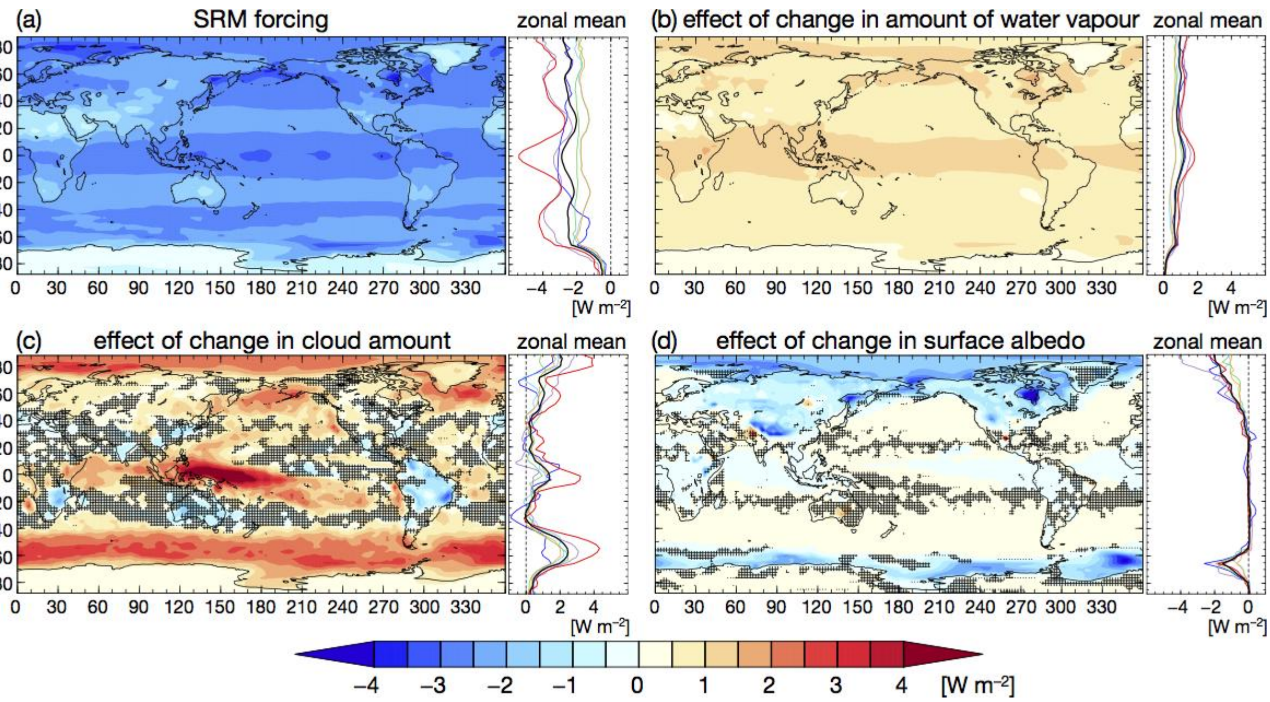

Figure 9. Same as Fig. 8 but for multi-model mean of (a) SRM forcing, SW feedback due to changes in the (b) water vapour amount, (c) cloud amount, and (d) surface albedo, averaged over 2040–2069.

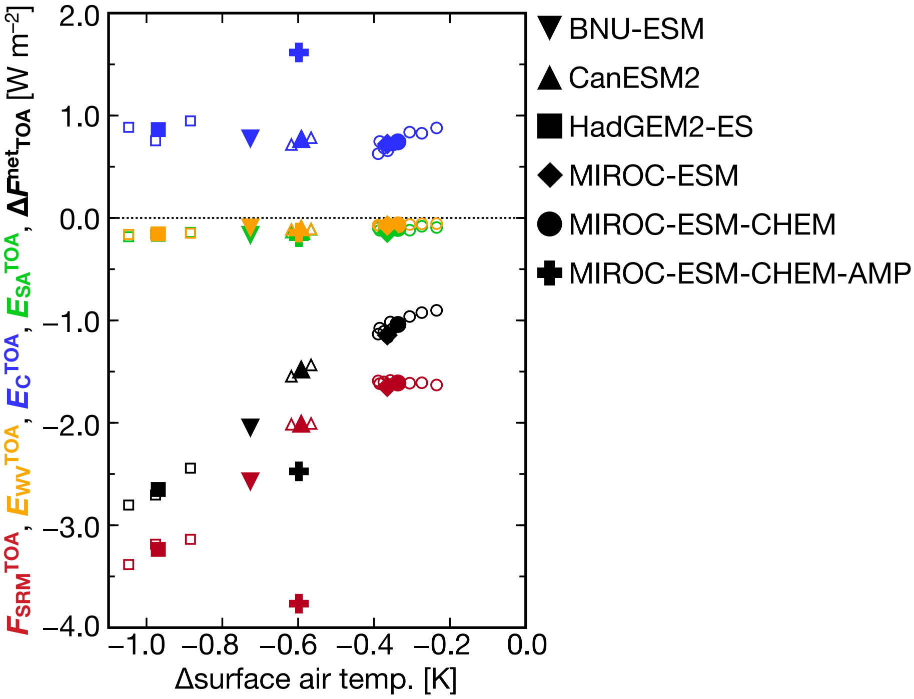

Figure 10. Same as Fig. 5 but the variables except for the surface temperature are calculated at the top of the atmosphere.

Table 1. Previous studies on simulation of sulphate geoengineering with calculation of stratospheric sulphate aerosols. Injected SO_2 amounts, baseline experiments, and model names are shown.

Studies	SO_2 [$\mathrm{Tg\,yr^{-1}}$]	Baseline experimets	Models
Rasch et al. (2008a)	2–4	doubled CO_2	CAM3
Robock et al. (2008)	3–10	A1B scenario	GISS GCM ModelE
Heckendorn et al. (2009), Pierce et al. (2010)	2–20	present day (year 2000)	MA-ECHAM4
Niemeier and Timmreck (2015)	2–200	RCP8.5 scenario	ECHAM5

Table 2. Models participating in GeoMIP G4 experiments and used in this study. Manners of simulating sulphate aerosol optical depth (AOD), particle sizes and standard deviation of their log-normal distribution (σ), and ensemble members are shown for each model.

Models	~~sulphate~~ Sulphate AOD	Particle size [µm] (σ)	Ensemble ~~Members~~ member
BNU-ESM Ji et al. (2014)	Prescribed	0.426 (1.25)	1
CanESM2 Arora and Boer (2010); Arora et al. (2011)	Uniform	0.350 (2.0)	3
HadGEM2-ES Collins et al. (2011)	Internally Calculated	0.0065 (1.3), 0.095 (1.4)	3
MIROC-ESM Watanabe et al. (2011)	Prescribed	0.243 (2.0)	1
MIROC-ESM-CHEM Watanabe et al. (2011)	Prescribed	0.243 (2.0)	9
MIROC-ESM-CHEM-AMP Watanabe et al. (2011); Sekiya et al. (2016)	Internally Calculated	0.243 (2.0)	1

Table 3. Values of rapid adjustment (Q_X) [$\mathrm{Wm^{-2}}$], feedback parameter ($-P_X$) [$\mathrm{Wm^{-2}K^{-1}}$], and correlation coefficient (R_X) due to changes in where $X =$ WV, C, SA. Multi-model means are also shown.

Models	Q_{WV}	$-P_{\mathrm{WV}}$	$\mathrm{R_{WV}}$	Q_{C}	$-P_{\mathrm{C}}$	$\mathrm{R_C}$	Q_{SA}	$-P_{\mathrm{SA}}$	$\mathrm{R_{SA}}$
BNU-ESM	0.32	−0.85	−0.93	~~0.69~~ 0.68	~~0.17~~ 0.14	~~0.11~~ 0.08	~~-5.4×10^{-2}~~ -4.2×10^{-2}	~~0.31~~ 0.33	~~0.52~~ 0.56
CanESM2	0.36	~~−0.77~~ −0.78	~~−0.74~~ −0.75	~~0.54~~ 0.53	~~−0.11~~ −0.12	−0.06	~~-7.9×10^{-3}~~ -9.0×10^{-3}	~~0.33~~ 0.32	~~0.66~~ 0.65
HadGEM2-ES	0.21	~~−0.99~~ −0.98	−0.97	~~1.23~~ 1.22	~~0.50~~ 0.49	~~0.41~~ 0.40	~~6.0×10^{-3}~~ 8.7×10^{-3}	~~0.24~~ 0.25	0.7
MIROC-ESM	0.20	−1.00	−0.90	1.06	~~1.43~~ 1.44	0.33	~~-1.1×10^{-2}~~ -9.9×10^{-3}	0.50	0.5
MIROC-ESM-CHEM	0.24	−0.90	~~−0.95~~ −0.96	0.73	~~0.15~~ 0.16	0.09	-3.5×10^{-3}	0.43	0.7
MIROC-ESM-CHEM-AMP	0.45	−0.95	−0.94	2.00	~~0.81~~ 0.85	~~0.36~~ 0.37	3.1×10^{-2}	0.44	~~0.68~~ 0.67
Multi-model mean	0.30	−0.91	−0.91	1.04	0.49	~~0.21~~ 0.20	~~-6.5×10^{-3}~~ -4.1×10^{-3}	0.38	0.6

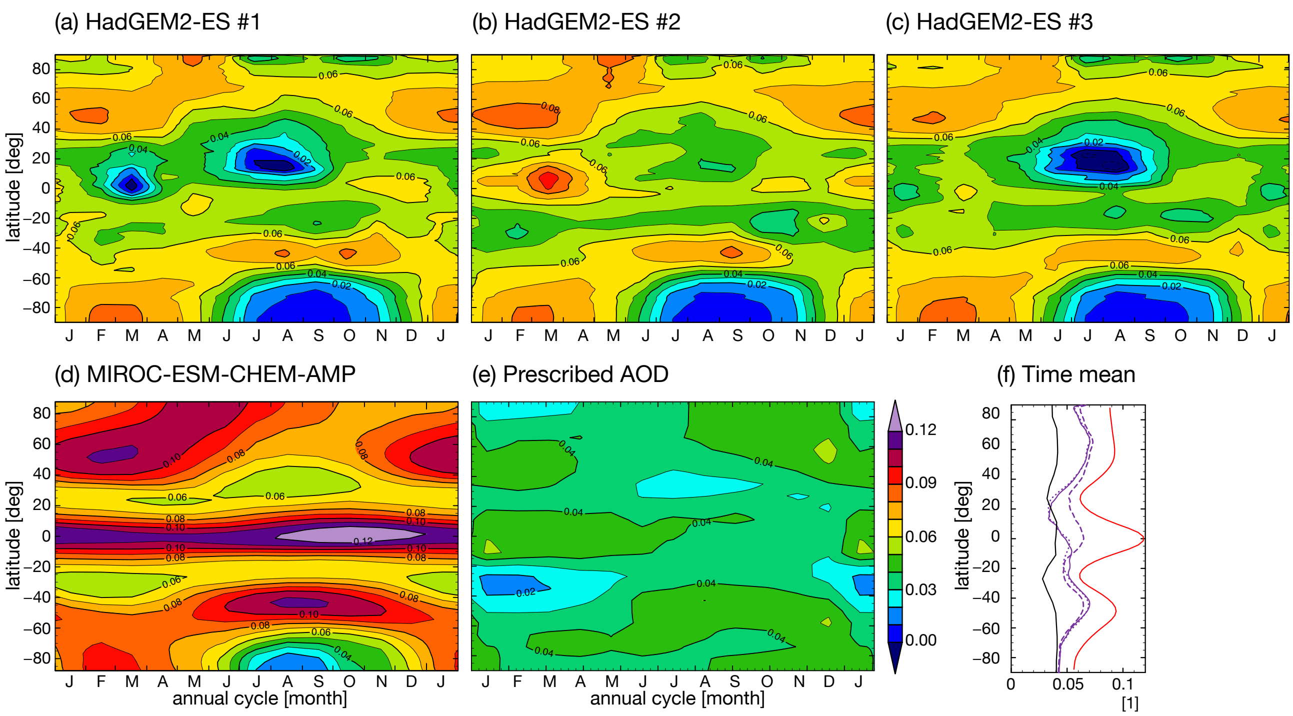

Figure S1. Annual cycle of stratospheric sulphate AOD averaged zonally and temporally over 2040–2069 for (a–c) each run of HadGEM2-ES and (d) MIROC-ESM-CHEM-AMP, (e) the prescribed AOD with same color shading, and (f) latitudinal distribution of the temporal means, where #1, #2, and #3 of HadGEM2-ES are shown by solid, dashed, and dotted purple lines, respectively, MIROC-ESM-CHEM-AMP by red line, and the prescribed AOD by black line. Note that HadGEM2-ES's AOD is approximately obtained by subtraction of sulphate aerosol AOD for both stratosphere and troposphere in G4 from that in RCP4.5.

Table S1. Same as Table 3 but for values at TOA.

Models	$Q_{\mathrm{WV}}^{\mathrm{TOA}}$	$-P_{\mathrm{WV}}^{\mathrm{TOA}}$	$\mathrm{R}_{\mathrm{WV}}^{\mathrm{TOA}}$	$Q_{\mathrm{C}}^{\mathrm{TOA}}$	$-P_{\mathrm{C}}^{\mathrm{TOA}}$	$\mathrm{R}_{\mathrm{C}}^{\mathrm{TOA}}$	$Q_{\mathrm{SA}}^{\mathrm{TOA}}$	$-P_{\mathrm{SA}}^{\mathrm{TOA}}$	$\mathrm{R}_{\mathrm{SA}}^{\mathrm{TOA}}$
BNU-ESM	1.4×10^{-2}	0.15	0.87	0.80	−0.01	−0.01	-3.1×10^{-2}	0.21	0.51
CanESM2	3.9×10^{-2}	0.12	0.63	0.56	−0.32	−0.18	-6.2×10^{-3}	0.22	0.63
HadGEM2-ES	-2.5×10^{-2}	0.14	0.90	1.28	0.36	0.32	1.4×10^{-3}	0.17	0.70
MIROC-ESM	1.2×10^{-2}	0.17	0.75	1.05	1.17	0.31	4.0×10^{-4}	0.37	0.52
MIROC-ESM-CHEM	-2.2×10^{-2}	0.14	0.85	0.73	−0.03	−0.02	6.3×10^{-4}	0.31	0.74
MIROC-ESM-CHEM-AMP	-3.7×10^{-2}	0.15	0.81	1.98	0.58	0.29	2.8×10^{-2}	0.32	0.67
Multi-model mean	-3.2×10^{-3}	0.15	0.80	1.07	0.29	0.12	-1.1×10^{-3}	0.27	0.63

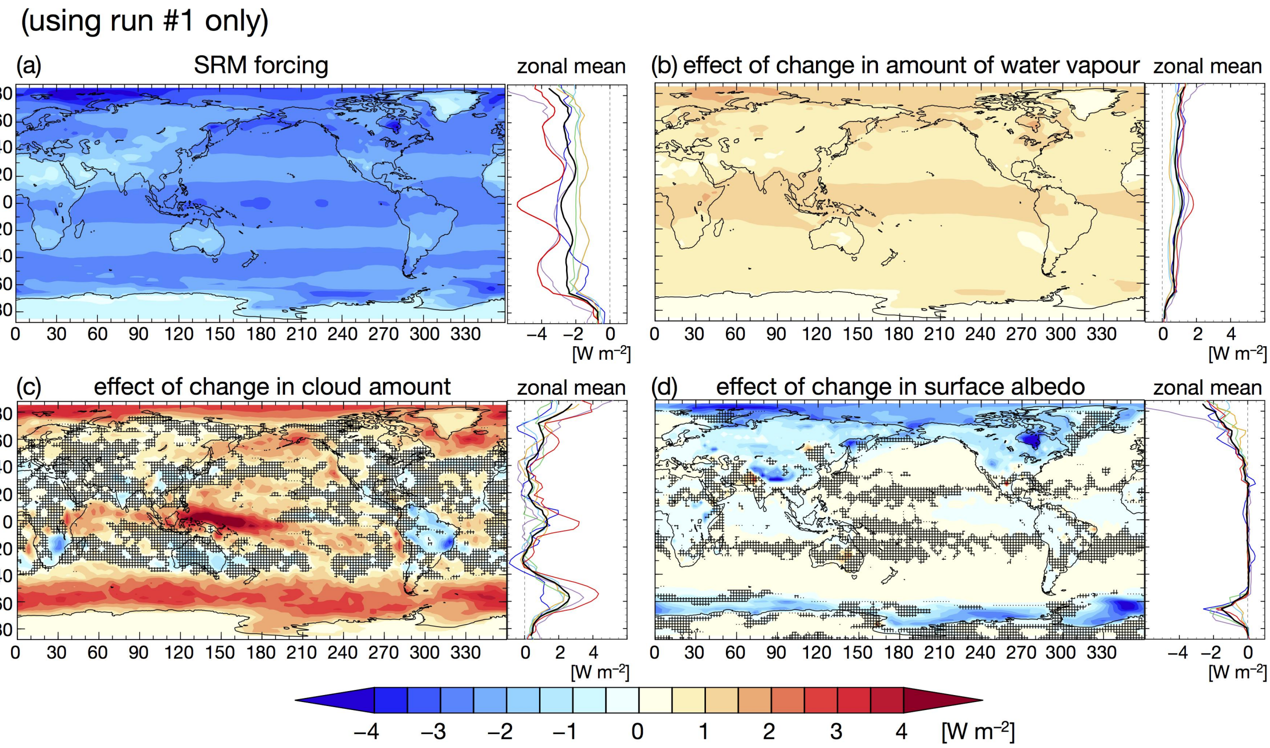

Figure S2. Same as Fig. 9 but using one run for each model.

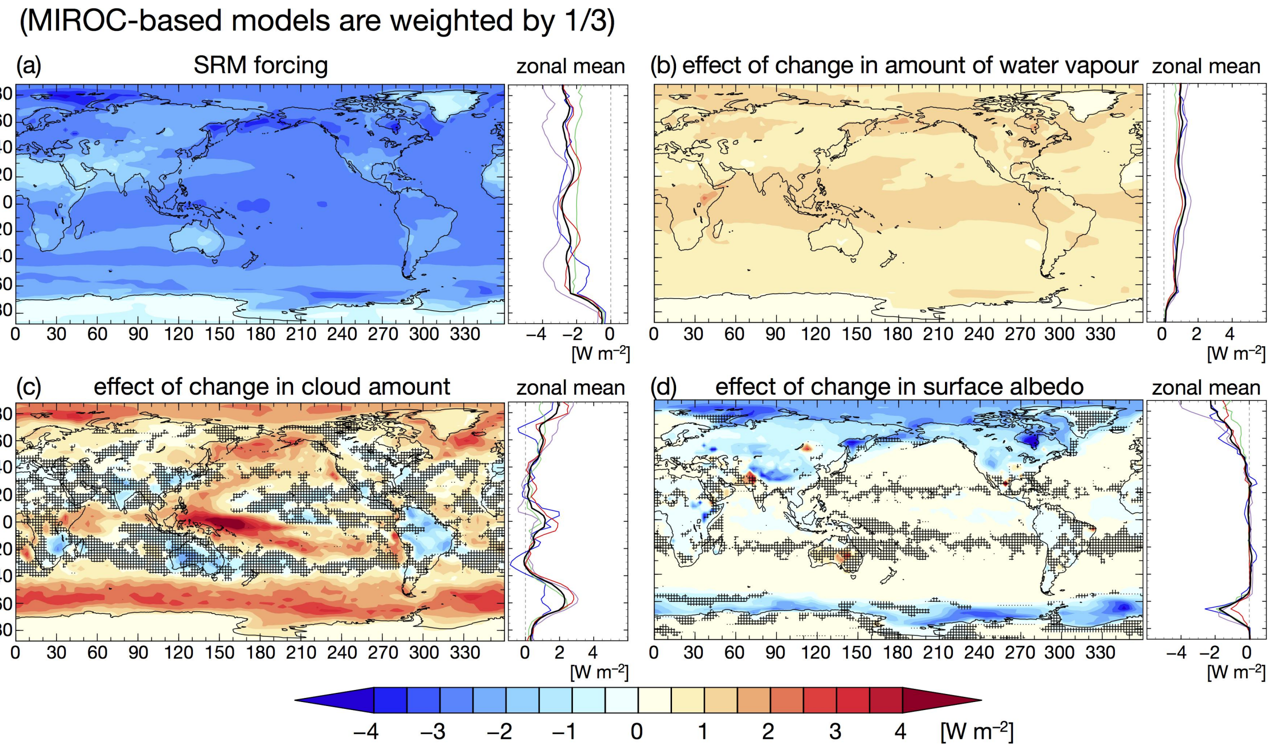

Figure S3. Same as Fig. 9 but the three MIROC-based models are weighted by 1/3 for the multi-model means and red lines indicate the means of the three MIROC-based models.